Chemical Geology 268 (2009) 27–40

Contents lists available at ScienceDirect

Chemical Geology

journal homepage: www.elsevier.com/locate/chemgeo

Nb/Ta fractionation observed in eclogites from the Chinese Continental Scientific Drilling Project

J.L. Liang [a], X. Ding [a], X.M. Sun [b], Z.M. Zhang [c], H. Zhang [a], W.D. Sun [a,d,*]

[a] CAS Key Laboratory of Isotope Geochronology and Geochemistry, Guangzhou Institute of Geochemistry, the Chinese Academy of Sciences, Guangzhou 510640, China
[b] Department of Earth Sciences, Sun Yat-Sen University, Guangzhou 510275, China
[c] Institute of Geology, Chinese Academy of Geological Sciences, Beijing 100037, China
[d] Research Center for Mineral Resources, School of Earth and Space Sciences, University Science and Technology of China, Hefei 230026, China

ARTICLE INFO

Article history:
Received 30 December 2008
Received in revised form 16 July 2009
Accepted 16 July 2009

Editor: R.L. Rudnick

Keywords:
Nb/Ta fractionation
Eclogite
Rutile
Amphibole
CCSD
Subduction

ABSTRACT

This paper reports detailed analyses of Nb and Ta concentrations of 19 eclogite samples and their principal mineral constituents from the main drill hole of the Chinese Continental Scientific Drilling Project (CCSD) and nearby outcrops. We observe highly fractionated and overall suprachondritic Nb/Ta values in minerals, e.g., rutile (4.8–87), titanite (12–62) and amphibole (2.0–67). Amphiboles in amphibolites (retrograded from eclogite) can be classified into two groups: a low Nb/Ta group that bears higher Al contents and is thus of higher pressure origin, and a high Nb/Ta, lower pressure group. The former group was likely formed during subduction; the latter may have formed during exhumation in the presence of rutile and titanite. The significant Nb/Ta fractionation in rutile and other minerals may reflect early dehydration of the subducted slab at shallow depths before the formation of rutile, which occurs at depths ≥50 km. The dehydration, with amphiboles existing as the main Nb–Ta-bearing phase, would lead to Nb/Ta fractionation, i.e., forming subchondritic Nb/Ta ratios in the released fluids and, complementarily, suprachondritic Nb/Ta ratios in the residual phases. While a large proportion of the fluids may escape from the slab to the mantle wedge, considerable amounts of the fluids can be retained in hydrous minerals within the descending slab, thus forming hydrated cold eclogites with subchondritic Nb/Ta characteristics. As subduction continues to depths over 50 km, rutile appears and consequently controls the Nb–Ta budget. In the presence of rutile, melting of the hydrated cold eclogites with very low Nb/Ta ratios would form magmas with negative Nb, Ta anomalies and subchondritic Nb/Ta. Further dehydration of the continuously descending slab results in even more fractionated Nb/Ta ratios in subsequently released fluids and residues, providing a feasible explanation for the large Nb/Ta variation observed in the modern arc magmas and residual eclogites.

© 2009 Elsevier B.V. All rights reserved.

1. Introduction

Niobium and Ta are usually taken as geochemically identical twins with the same valence state (+5) and similar atomic radii (~0.64 Å) for octahedral coordination (Shannon, 1976). Although the ionic radii of Nb is actually slightly larger than that of Ta (Tiepolo et al., 2000), they are not fractionated dramatically from each other in most mantle magmatic processes (Jochum et al., 1986; Jochum et al., 1989; Sun and McDonough, 1989; Rudnick et al., 2000). All the reservoirs of the silicate Earth sampled so far (continental crust, IAB, MORB, OIB, etc.), however, display subchondritic or chondritic Nb/Ta ratios (Jochum et al., 1986; Sun and McDonough, 1989; Mcdonough and Sun, 1995; Niu and Batiza, 1997; Barth et al., 2000; Munker et al., 2003; Sun et al., 2003), indicating a missing reservoir with suprachondritic Nb/Ta exists somewhere (Rudnick et al., 2000). It has been proposed that the missing Nb may be stored in the core, due to the siderophile property of Nb at high pressure and extremely low oxygen fugacity (Wade and Wood, 2001). However, Nb concentrations are very low in the metal phase of the Grant, Toluca and Canyon Diablo iron meteorites (Kamber et al., 2003). Therefore, it is still not clear whether the missing Nb is indeed stored in the core.

Alternatively, it has been proposed that rutile-bearing eclogites can account for the Nb and Ta depletion in the continental crust and mantle (Kamber and Collerson, 2000; Rudnick et al., 2000). This model is supported by highly fractionated and overall suprachondritic Nb/Ta of rutile grains in eclogitic xenoliths of kimberlite from the western Africa and Siberia cratons (Rudnick et al., 2000) and highly fractionated Nb/Ta in ultra high pressure metamorphism (UHPM) eclogites from the CCSD drill hole (Xiao et al., 2006).

Rutile is the most important titanium-bearing phase responsible for the distribution and budget of high field strength elements (HFSEs), especially Nb, Ta and Ti in subduction zone settings (Brenan et al., 1994; Green, 1995). Given that rutile favors Ta over Nb (Foley

* Corresponding author. CAS Key Laboratory of Isotope Geochronology and Geochemistry, Guangzhou Institute of Geochemistry, the Chinese Academy of Sciences, Guangzhou 510640, China. Tel.: +86 20 85290215; fax: +86 20 85291510.
E-mail address: weidongsun@gig.ac.cn (W.D. Sun).

0009-2541/$ – see front matter © 2009 Elsevier B.V. All rights reserved.
doi:10.1016/j.chemgeo.2009.07.006

et al., 2000; Horng and Hess, 2000; Foley et al., 2002; Schmidt et al., 2004; Klemme et al., 2005b; Xiong et al., 2005; Bromiley and Reffern, 2008; Klimm et al., 2008), partial melting and dehydration of the subducting slab in the presence of rutile decreases the Nb/Ta in the residual phases. Moreover, because rutile controls the Nb and Ta budgets (most of the Nb and Ta are hosted in rutile), Nb and Ta will not dramatically fractionate from each other in the presence of rutile. Given that the formation of the continental crust requires rutile as a residual phase (McDonough, 1991; Rapp et al., 2003; Xiong et al., 2006), major fractionation of Nb/Ta before rutile appears is essential to form the continental crust (Xiao et al., 2006) with Nb, Ta and Ti depletions and low Nb/Ta ratios of 12–13 (Rudnick, 1995; Barth et al., 2000; Rudnick et al., 2000).

Highly fractionated and overall subchondritic Nb/Ta have been reported for rutile from CCSD drill hole samples, which has been interpreted in the context of a "zone refining" dehydration model (Xiao et al., 2006). According to the model, Nb/Ta fractionation occurs at shallow depths in the absence of rutile during blueschist-to-amphibolite transformation (Xiao et al., 2006), resulting in low Nb/Ta in hydrous eclogites in cold regions with complementary high Nb/Ta in hot regions (Xiao et al., 2006). The investigated rutile grains, however, were collected from only one of the pilot drill holes at a depth of about 180 m. The proposed suprachondritic Nb/Ta in hotter regions was not reported. In this paper, we studied 19 eclogite samples from 100 to 3000 m depths in the main drill hole of the CCSD, a pilot drill hole, and several field outcrops. Major and trace elements (especially Nb, Ta and Ti) in bulk rock and their minerals (including rutile, titanite, amphibole, phengite, garnet, omphacite, apatite and epidote) were analyzed. Our results strongly support major Nb/Ta fractionation and suprachondritic Nb/Ta in residual eclogites.

2. Geological setting and CCSD

The CCSD project, started in June 2001 and ended in January 2005, aimed to reconstruct the formation and exhumation mechanisms of the Dabie–Sulu UHP terrane in eastern China (Xu, 2004). It consists of several pilot drill holes and a main drill hole of 5158 m. The main drill hole is located in Donghai (at 34°25′N, 118°40′E) (Fig. 1A) on the south limb of the Sulu UHP metamorphic belt, the eastern end of the Qinling–Dabie–Sulu orogenic belt, which is the main suture between the North and South China blocks (Meng and Zhang, 1999, 2000; Sun et al., 2002a; Zheng et al., 2003). It is famous for Triassic deep continental subduction (Ames et al., 1996; Li et al., 2000; Sun et al., 2002a, 2002b; Liu et al., 2006), and associated UHP minerals, such as coesite and micro-diamonds (Wang et al., 1989; Wang and Liou, 1991; Xu et al., 1992; Ye et al., 2000; Xu et al., 2003; Zhang et al., 2003).

The region near the main drill hole is underlain mainly by orthogneiss and supracrustal rocks (including paragneiss, jadeite-bearing quartzite, marble and mica schist) intruded by Cretaceous granite and unconformably overlain by Quaternary sedimentary cover. More than one hundred outcrops of eclogite were found in Donghai, and occurred as pods or layers in gneiss ranging from <1 m to hundreds of meters in length. The lithologies in the drill core are similar to those exposed in the field outcrops (Liu et al., 2004; Xu, 2004; Zhang et al., 2004, 2008). The main hole consists mainly of eclogite (around 1300 m, 26.6%), paragneiss (around 1400 m, 28%),

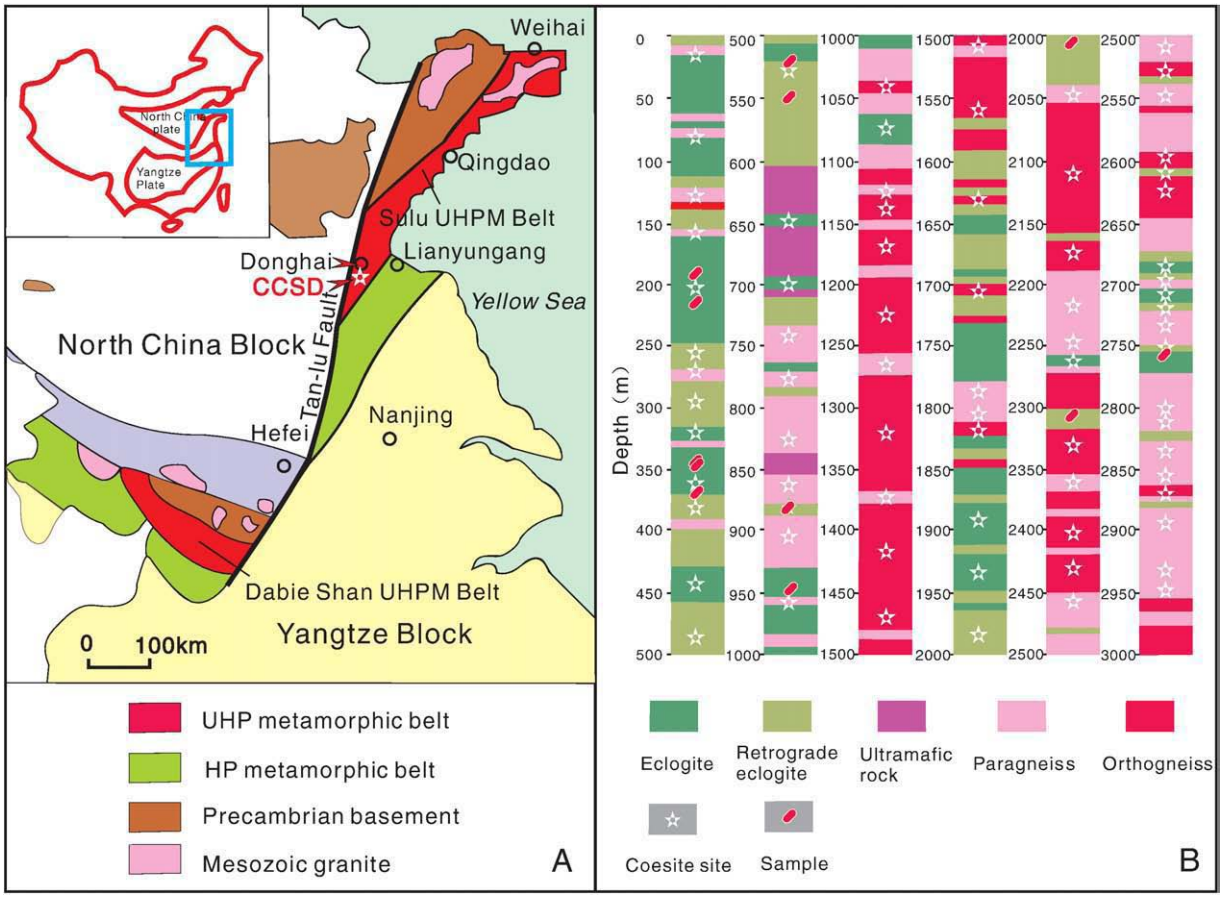

Fig. 1. (A) Simplified geological map of the Dabie–Sulu orogenic belt showing the location of CCSD (Modified after Xiao et al., 2006). (B) Simplified lithological profile of the main drill hole core of CCSD.

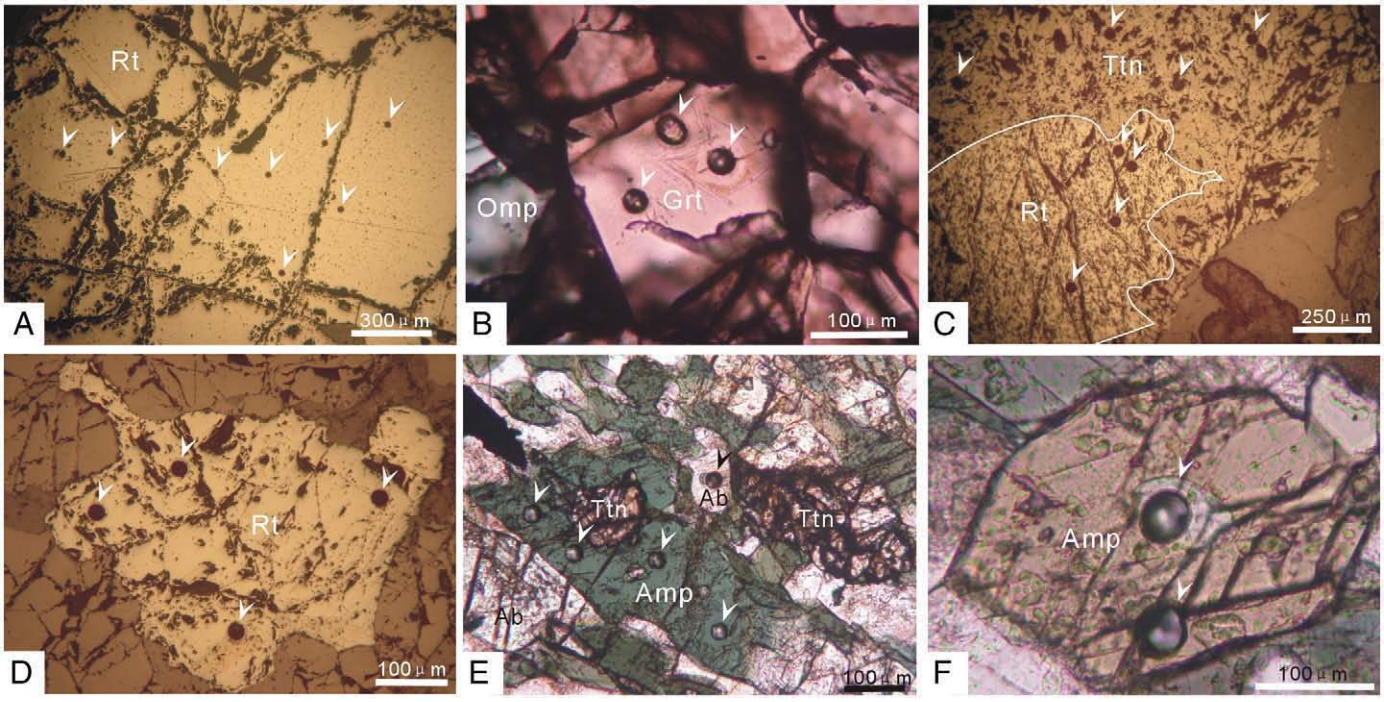

Fig. 2. Optical microphotographs of minerals in eclogite from CCSD show the laser ablation pits. (Rt, rutile; Omp, omphacite; Grt, garnet; Ttn, titanite; Amp, amphibole; Ab, albite). In some cases, rutile retrogrades to titanite.

orthogneiss (around 2100 m, 44%) and ultramafic rocks (around 70 m, 1.4%) (Zhang et al., 2004; Xu, 2007). An UHPM index mineral, coesite, was discovered in many sections of the main hole (Fig. 1B). Quartz veins in UHP metamorphic rocks are widely mined in the region (Xu et al., 2005). Highly oxidized minerals found in quartz veins indicate that high-SiO_2 fluids may have acted as oxidizing agents, which explains the high oxygen fugacity at convergent margins (Sun et al., 2007). Rutile in eclogite is abundant near the CCSD, which is part of a large rutile deposit (Xu et al., 2004; Chen et al., 2005).

3. Samples and analytical methods

All together, 19 eclogites were collected from the upper part of the main drill hole core (from 100 to 3000 m) (Fig. 1B), a pilot hole, several field outcrops in Maobei, Qinglongshan, Tuofeng, Sanqingge, and a rock-collecting pit near the main hole in Donghai. Samples were cut and polished into thin sections with thicknesses from 0.2 to 0.5 mm. Fresh eclogite consists mainly of garnet and omphacite as main phases and rutile, quartz, phengite, apatite, epidote, and kyanite as accessory phases. UHPM index minerals of coesite and micro-diamonds occur as inclusions in garnet, omphacite, zircon or epidote (Xu et al., 1992, 2003). Rutile in retrograded eclogites has thin ilmenite and/or titanite overgrowths. Similarly, garnet and omphacite are rimmed by symplectite of plagioclase and pargasite. In some places, eclogite was totally replaced by amphibolite, while rutile retrograded to titanite (Fig. 2).

The major and trace elements of the bulk rock samples were analyzed at the Chinese Academy of Sciences (CAS) Key Laboratory of Isotope Geochronology and Geochemistry, Guangzhou Institute of Geochemistry. Eclogite samples were first powdered in an agate mill to less than 200 mesh, and then fluxed with $Li_2B_4O_7$ to make homogeneous glasses at 1150–1200 °C using a V8C automatic fusion machine produced by Analymate Company in China. The bulk rock major elements were analyzed by X-ray fluorescence spectrometry (Rigaku 100e), with a sample/flux ratio of 1:8. Analytical precision and accuracy for major elements were better than 1% (Ma et al., 2007). Trace elements were determined by laser ablation (LA)-ICP-MS, using fluxed glasses with a sample/flux ratio of 1:3. The LA-ICP-MS system consists of an Agilent 7500a ICP-MS coupled with a Resonetics RESOLution M-50 ArF-Excimer laser source ($\lambda = 193$ nm). Laser energy was 80 mJ, and frequency was 10 Hz with ablation spot of 69 μm in diameter. Both double-volume sampling cell and Squid pulse smoothing device were used to improve the data quality (Tu et al., 2009). The ablated aerosol was carried to the ICP source with He gas. NIST 612 was used as an external calibration standard, and ^{43}Ca as the internal standard. The reference values of NIST 612 are in Table 1 (Pearce et al., 1997). The detection limits of ICP-MS for trace elements are mostly better than 10 ppb, with uncertainties of 5–10%.

The major and minor element compositions of rutile, titanite and silicate minerals in eclogite (and its retrograded products, amphibolite) were analyzed using a JXA-8800R electron microprobe equipped with wavelength dispersive spectrometers (WDS) and energy dispersive spectrometer (EDS) at Sun Yat-Sen University. Operating conditions were 15.0 kV accelerating voltage, 20 nA beam current and 10 μm electron beam diameter. Both silicate minerals and pure oxides were used as standards (Liang et al., 2006).

The trace element concentrations of minerals were measured *in situ* at the National Key Laboratory of Continental Dynamics, Northwest University, Xi'an, using LA-ICP-MS. The system consists of an

Table 1
The reference values and analyzed values of international reference materials used for calculation (ppm).[a]

Element		Ti	V	Cr	Zr	Nb	Hf	Ta	U
NIST 610		434	441.7	405.2	439.9	419.4 (485)[b]	417.7	376.6 (482)[b]	457.1
NIST 612		48.11	39.22	39.88	35.99	38.06	34.77	39.77	37.15
KL2-G	*R*	2.56[c]	309	294	152	15.0	3.93	0.961	0.548
	A	2.95[c]	317	338	135	14.0	3.44	0.91	0.54
ML3B-G	*R*	2.13[c]	268	177	122	8.61	3.22	0.555	0.442
	A	2.65[c]	300	195	117	8.26	3.05	0.54	0.44

R – The reference values from Jochum et al. (2006); *A* – The analyzed values.
[a] The reference values of NIST 610 and NIST 612 from Pearce et al., 1997.
[b] The values of Nb and Ta of NIST 610 from Hu et al. (2008).
[c] The values of TiO_2 in wt.%.

Table 2
Major and trace elements compositions of eclogites from CCSD.

Sample	04303	04304	06022	04307	04308	03558	03564	03568	04313	04314
Depth (m)	193	218	340	343	360	370	521	881	952	1082
By XRF (wt.%)										
SiO_2	49.9	57.1	57.6	41.7	45.5	56.1	50.4	47.2	50.3	52.5
TiO_2	1.73	1.32	2.14	5.93	0.940	1.41	2.59	1.95	1.52	1.09
Al_2O_3	13.9	13.6	13.7	13.5	13.4	13.9	15.5	16.8	16.0	16.7
$Fe_2O_3^{total}$	13.8	10.5	11.8	20.1	17.8	10.2	11.00	14.8	12.1	10.8
MnO	0.20	0.150	0.230	0.300	0.180	0.190	0.260	0.270	0.150	0.150
MgO	5.30	4.91	3.54	5.46	7.19	4.06	5.98	4.66	6.27	6.30
CaO	10.1	7.84	5.24	9.47	11.4	7.23	11.1	9.76	8.45	8.64
Na_2O	3.90	2.57	2.09	2.78	3.10	3.28	2.850	3.28	3.07	1.93
K_2O	0.240	1.32	2.23	0.030	0.030	1.94	0.081	0.390	1.14	0.230
P_2O_5	0.300	0.200	0.910	0.230	0.050	0.640	0.160	0.190	0.400	0.400
L.O.I	0.260	0.340	0.250	0.180	0.230	0.830	−0.100	0.160	0.130	1.08
Total	99.6	99.8	99.8	99.7	99.8	99.8	99.7	99.5	99.6	99.7
By LA-ICP-MS (ppm)										
P	1857	1193	4748	1297	321	3423	2525	906	1962.	2069
Sc	51.5	38.0	29.5	89.0	414	31.6	42.4	44.9	28.2	27.7
Ti	12,623	8667	13,726	41,128	6753	9240	14,139	12,108	10,715	7495
V	412	255	133	610	359	185	276	237	221	145
Cr	175	349	289	127	345	237	216	277	348	120
Co	61.6	32.6	19.5	38.4	50.7	26.9	45.3	30.2	38.3	29.1
Ni	89.9	131	116	54.5	81.8	106	86.0	82.1	149	49.6
Cu	225	33.4	33.8	20.0	226	128	847	138	108	1463
Ga	19.4	15.3	13.5	15.6	15.0	16.2	18.7	15.3	16.6	13.1
Rb	3.57	28.7	47.2	1.01	0.900	25.7	23.8	3.49	15.6	5.12
Sr	191	111	105	77.7	110	219	303	104	164	829
Y	34.0	23.1	37.4	24.1	12.6	34.0	37.4	63.2	24.0	20.8
Zr	164	99.2	373	16.6	13.1	161	189	163	155	128
Nb	4.25	2.15	4.15	2.79	0.950	5.73	6.460	7.28	4.58	4.36
Mo	1.23	1.44	1.17	1.55	0.770	1.62	1.07	0.990	0.940	1.30
Sn	1.71	1.31	0.970	1.55	1.73	2.30	4.46	2.44	0.990	8.37
Cs	0.080	0.790	0.900	0.070	0.090	1.01	0.330	0.03	0.550	0.240
Ba	361	472	316	18.0	58.9	564	646	52.5	350	104
La	13.1	12.1	12.7	4.59	1.91	54.1	9.35	6.20	27.3	23.6
Ce	35.5	29.69	33.6	12.5	4.49	122.9	21.9	18.2	57.2	46.7
Pr	5.35	4.02	4.93	1.95	0.800	15.6	3.08	2.88	7.28	5.93
Nd	27.4	18.4	23.9	10.21	4.46	67.7	15.3	14.6	31.0	25.5
Sm	6.92	4.21	5.78	3.31	1.86	14.1	4.71	5.10	5.82	5.18
Eu	2.37	1.37	2.09	1.47	0.800	3.31	1.78	1.59	1.99	1.74
Gd	6.58	4.22	6.38	4.27	2.44	10.9	6.51	8.24	5.12	4.66
Tb	0.950	0.660	0.960	0.720	0.400	1.26	1.05	1.56	0.750	0.650
Dy	6.35	4.27	6.92	4.71	2.51	6.70	7.12	10.7	4.60	4.01
Ho	1.30	0.900	1.48	0.930	0.530	1.26	1.43	2.21	0.920	0.820
Er	3.79	2.56	4.38	2.54	1.42	3.49	4.12	6.31	2.71	2.23
Tm	0.56	0.37	0.660	0.350	0.220	0.510	0.580	0.910	0.390	0.330
Yb	3.63	2.45	4.81	2.24	1.23	3.29	3.78	5.69	2.48	2.08
Lu	0.560	0.370	0.830	0.330	0.200	0.510	0.590	0.830	0.37	0.330
Hf	3.89	2.51	7.96	0.54	0.55	4.06	4.58	3.99	3.75	3.11
Ta	0.239	0.169	0.314	0.113	0.110	0.320	0.404	0.355	0.241	0.254
Pb	2.28	3.50	3.96	3.01	11.33	4.89	20.3	2.29	2.90	35.9
Th	0.960	0.740	2.00	0.830	0.610	2.84	0.570	0.290	1.58	1.83
U	0.320	0.330	0.400	0.450	0.230	1.41	0.240	0.350	0.190	0.260
Nb/Ta	17.8	12.7	13.3	24.6	8.66	17.9	16.00	20.5	19.0	17.2

Sample	04319	04320	04325	03530	05013	03552	05016	05022	03550
Depth (m)	2007	2032	2317	Tuofeng	Maobei	Maobei	Qinglongshan	Qinglongshan	Sanqingge
By XRF (wt.%)									
SiO_2	47.1	49.9	50.1	47.4	46.7	40.9	50.0	45.8	41.6
TiO_2	1.32	1.65	1.36	1.66	0.790	3.07	1.25	1.26	1.09
Al_2O_3	16.4	15.2	15.5	16.7	16.5	15.9	17.5	19.3	15.2
$Fe_2O_3^{total}$	12.4	11.7	11.1	13.9	12.9	20.6	11.4	13.5	10.1
MnO	0.180	0.170	0.160	0.260	0.180	0.190	0.150	0.200	0.140
MgO	7.45	6.31	6.16	7.44	7.61	5.22	5.32	5.60	5.24
CaO	10.2	8.57	8.80	9.28	11.1	11.5	9.81	9.66	15.7
Na_2O	2.94	2.73	3.58	1.80	3.36	1.82	2.63	3.33	1.61
K_2O	0.820	1.22	1.57	0.450	0.020	0.010	0.430	0.030	0.680
P_2O_5	0.110	0.360	0.260	0.240	0.000	0.140	0.370	0.250	0.290
L.O.I	0.670	1.88	1.10	0.470	0.500	0.380	0.690	0.650	8.79
Total	99.6	99.7	99.7	99.5	99.6	99.8	99.7	99.5	100
By LA-ICP-MS (ppm)									
P	602	719	1336	1304	62.0	831	1010	1149	3287
Sc	37.3	45.3	32.5	46.1	41.6	60.9	19.7	36.1	54.2
Ti	8847	14,074	8884	10,293	5775	23,306	5017	8522	13,055

Table 2 (*continued*)

Sample	04319	04320	04325	03530	05013	03552	05016	05022	03550
Depth (m)	2007	2032	2317	Tuofeng	Maobei	Maobei	Qinglongshan	Qinglongshan	Sanqingge
By LA-ICP-MS (ppm)									
V	239	468	221	209	270	529	89.9	135	388
Cr	332	5.86	336	277	345	26.5	234	174	280
Co	33.6	38.7	41.2	37.9	40.9	50.7	24.6	52.1	51.2
Ni	125	24.2	141	104	140	19.3	56.4	79.3	92.9
Cu	50.3	1095	99.0	50.7	30.0	101	29.5	69.3	141
Ga	14.9	15.5	16.3	11.6	17.2	15.2	9.15	16.1	27.8
Rb	20.7	2.57	32.7	7.92	1.47	0.520	9.10	1.53	6.79
Sr	99.0	82.3	236	98.5	45.1	61.9	55.9	733	1525
Y	24.6	21.2	29.5	27.8	10.6	11.4	15.6	14.6	28.7
Zr	88.8	44.8	120	75.1	7.24	12.9	70.9	76.9	165
Nb	3.12	2.46	3.87	4.22	0.240	0.500	2.36	2.54	4.06
Mo	0.840	0.900	0.960	0.630	1.30	0.840	0.260	0.500	0.730
Sn	1.01	5.74	1.61	1.32	1.02	1.12	0.640	0.820	1.56
Cs	0.100	0.110	0.490	0.420	0.090	0.070	0.550	0.100	0.820
Ba	169	320	333	488	6.60	14.8	265	72.7	783
La	8.08	5.76	5.17	4.13	0.800	4.37	9.32	13.6	32.5
Ce	17.5	12.5	13.9	10.3	1.25	10.6	19.2	28.6	67.0
Pr	2.23	1.71	2.16	1.43	0.150	1.72	2.61	3.61	8.37
Nd	9.93	8.42	11.6	7.14	1.02	8.89	11.7	16.6	37.5
Sm	2.81	2.66	3.98	2.05	1.07	2.82	2.80	3.30	7.69
Eu	1.16	1.05	1.22	1.17	0.610	1.14	0.970	1.26	2.83
Gd	4.00	3.52	5.50	3.58	1.80	2.80	2.89	2.97	7.41
Tb	0.670	0.580	0.890	0.660	0.280	0.390	0.420	0.420	0.970
Dy	4.67	3.86	5.63	5.28	1.89	2.42	2.59	2.72	5.70
Ho	0.940	0.810	1.08	1.10	0.440	0.470	0.510	0.540	1.12
Er	2.68	2.34	3.06	3.05	1.16	1.25	1.48	1.64	2.94
Tm	0.380	0.350	0.430	0.460	0.160	0.160	0.200	0.260	0.410
Yb	2.54	2.19	2.87	3.16	1.09	1.00	1.30	1.56	2.62
Lu	0.360	0.320	0.420	0.480	0.150	0.150	0.200	0.220	0.400
Hf	2.22	1.12	3.10	1.98	0.280	0.450	1.69	1.66	4.01
Ta	0.156	0.162	0.232	0.216	0.020	0.034	0.104	0.104	0.197
Pb	2.61	23.0	5.54	3.91	0.510	5.36	1.19	7.08	6.70
Th	0.550	0.580	0.450	0.420	0.010	0.570	0.250	0.610	2.18
U	0.110	0.290	0.290	0.180	0.050	0.430	0.240	0.190	0.340
Nb/Ta	19.9	15.1	16.7	19.5	12.1	14.8	22.8	24.5	20.6

Agilent 7500a ICP-MS coupled with a GeoLas 200M ArF-Excimer laser source ($\lambda = 193$ nm, beam frequency is 20 Hz, beam energy is 200 mJ). Ablation spots were 30–60 μm depending on the size of the grain, with ablation depths of 20–40 μm. The ablated aerosol was carried to the ICP source with He gas. ^{49}Ti was used as an internal standard for rutile and titanite, ^{43}Ca for apatite, and ^{29}Si for silicate minerals, respectively (Yuan et al., 2004). NIST 610 was used as an external calibration standard (Table 1) (Pearce et al., 1997). The Nb and Ta values for NIST 610 from the recent literature were used for calculation of the concentration in the unknowns (Hu et al., 2008). The trace element concentrations were calculated using GLITTER Version 4.0. Reproducibility and accuracy of trace element concentrations were better than 10% (see Liu et al., 2002 for more detailed information). The mean detection limits of the elements determined for all minerals were Ti = 0.95 ppm, Zr = 0.09 ppm, Nb = 0.027 ppm, Hf = 0.12 ppm, Ta = 0.01 ppm, and U = 0.014 ppm.

4. Results

The major and trace elements of bulk rocks are listed in Table 2, and the compositions of rutile, titanite, apatite, garnet, omphacite, phengite, epidote and amphibole in fresh eclogite, retrograded eclogite and amphibolite (the retrograded product of eclogite) are listed in Table 3. Trace elements of rutile and other minerals above are listed in Tables 4 and 5, respectively.

4.1. Ti, Nb and Ta in eclogite

The content of Ti in bulk eclogite varies dramatically (Table 2). Titanium is weakly positively correlated with Nb, and Ta (with $R^2 = 0.346$, 0.432 respectively, Fig. 3A, B). No obvious correlation between Nb/Ta and Ti, Nb/Ta in rutile and host eclogite was observed (Fig. 3C, D). Overall, half of the eclogite samples have superchondritic Nb/Ta, the rest are subchondritic (Fig. 3C).

Two fresh eclogite samples were selected to calculate the mass balance between minerals and the whole rock. The retrograded eclogites and amphibolites were not selected for this purpose, because retrograde alteration makes it difficult to estimate mineral modes. We calculated the contributions of each mineral to the whole rock for Ti, Nb, Ta, Zr and Hf. The result indicates that more than 90% of Ti, Nb and Ta are hosted by rutile, while 30–70% of Zr and Hf are hosted in rutile (Table 6).

4.2. Nb and Ta in rutile and titanite

As shown in Table 4, both Nb and Ta concentrations and Nb/Ta vary dramatically in rutile. Nb concentrations range from 8.4 to 1121 ppm, Ta from 0.2 to 96 ppm. Correspondingly, Nb/Ta varies from 4.8 to 87; about 63.5% of the data points have suprachondritic Nb/Ta ratios (Figs. 4 and 5A). The correlations between Nb and Nb/Ta displayed two opposite trends: negative correlations (Fig. 5A, B, D) and positive correlations (Fig. 5C), indicating that the fractionation between Nb and Ta was controlled by at least two major processes (see details below).

Similar to the results of previous studies, Nb and Ta concentrations and Nb/Ta also vary significantly between different grains from the same sample and even within the same grain (Xiao et al., 2006). For example, Nb/Ta ranges from 22 to 87, with Nb concentrations from 31 ppm to 182 ppm in one rutile grain in sample 03552, and Nb/Ta is positively correlated with Nb (Fig. 5C). By contrast, sample 06018 has much lower Nb/Ta, ranging from 7.3 to 18, with weak negative correlation between Nb and Nb/Ta (Fig. 5B). The highest concentrations

Table 3
Representative major and minor element composition of minerals in eclogites from CCSD (wt.%).

Sample	03568		03550		04307	04325		04320	04325	04342	05016	06018
Location [a]	881m		SQG		343m	2317m		2033m	2317m	2762m	QLS	550m
Minerals [b]	Grt(r)	Grt(c)	Omp(r)	Omp(c)	Rt(16)	Ttn-1	Ttn-2	Amp(9)	Amp(9)	Phn(10)	Epi(8)	Ap(6)
SiO_2	39.3	39.0	55.6	55.8	0.002	30.4	29.9	42.3	42.9	54.5	38.1	0.002
TiO_2	0.020	0.080	0.080	0.060	99.5	39.2	37.4	0.610	0.580	0.440	0.050	0.010
Al_2O_3	21.4	21.0	9.52	9.46	0.000	0.930	1.65	12.5	11.5	23.5	26.6	0.001
Cr_2O_3	0.001	0.010	0.030	0.010	0.070	0.040	0.010	0.03	0.020	0.040	0.030	nd
FeO^{total}	23.7	23.7	6.59	6.25	0.370	0.330	0.560	16.6	16.0	1.79	9.60	0.010
MnO	0.800	0.710	0.090	0.070	0.001	0.090	0.060	0.460	0.340	0.000	0.050	0.030
MgO	4.76	4.75	7.78	7.53	0.001	0.030	0.001	10.4	10.9	5.20	0.410	0.010
CaO	10.7	11.6	12.2	12.3	0.030	28.9	28.8	11.4	11.4	0.040	21.9	57.7
Na_2O	0.050	0.070	7.33	7.09	0.000	0.000	0.000	1.74	1.57	0.070	0.030	0.010
K_2O	0.001	0.002	0.002	0.010	0.010	0.020	0.010	1.13	1.01	9.91	0.003	0.010
P_2O_5	nd	nd	nd	nd	nd	nd	nd	nd	nd	nd	nd	40.7
F	nd	nd	nd	nd	nd	nd	nd	nd	nd	nd	nd	2.68
Total	100	100	99.2	98.5	99.9	99.9	98.3	97.0	96.2	95.5	96.8	99.9
O	12	12	6	6	2	5	5	23	23	12	12.5	12
Si	3.03	3.02	2.02	2.03	0.000	0.990	0.990	6.40	6.53	3.92	3.06	0.000
Ti	0.000	0.000	0.000	0.000	1.00	0.970	0.940	0.070	0.070	0.020	0.000	0.000
Al	1.94	1.91	0.410	0.410	0.000	0.040	0.060	2.23	2.07	1.99	2.52	0.000
Cr	0.000	0.000	0.000	0.000	0.000	0.000	0.000	0.000	0.000	0.000	0.000	0.000
Fe^{3+}	0.010	0.000	0.000	0.000	0.000	0.000	0.000	0.020	0.000	0.010	0.020	0.00
Fe^{2+}	1.52	1.53	0.200	0.190	0.000	0.010	0.020	2.08	2.03	0.100	0.630	0.00
Mn	0.050	0.050	0.000	0.000	0.000	0.000	0.000	0.060	0.040	0.000	0.000	0.000
Mg	0.550	0.550	0.420	0.410	0.000	0.000	0.000	2.34	2.46	0.560	0.050	0.000
Ca	0.890	0.960	0.470	0.480	0.000	1.01	1.03	1.84	1.85	0.000	1.89	5.01
Na	0.010	0.010	0.520	0.500	0.000	0.000	0.000	0.510	0.460	0.010	0.000	0.000
K	0.000	0.000	0.000	0.000	0.000	0.000	0.000	0.220	0.200	0.910	0.000	0.000
P	nd	nd	nd	nd	nd	nd	nd	nd	nd	nd	nd	2.79
F	nd	nd	nd	nd	nd	nd	nd	nd	nd	nd	nd	0.650

nd – not determined.
[a] The number with the unit of meter is the depth of the main hole of CCSD, SQG – Sanqingge outcrop eclogite, QLS – Qinglongshan outcrop eclogite.
[b] r – rim, c – core, the number in the bracket is the analysis points, Grt – garnet, Omp – omphacite, Rt – rutile, Ttn – titanite, Amp – amphibole, Phn – phengite, Epi – epidote, Ap – apatite.

of Nb were observed in samples 03530 and 04342, with mean Nb concentration and Nb/Ta values of 1121 ppm, 12, and 1080 ppm, 18, respectively. All these facts indicate strong fractionation between Nb and Ta and inhomogeneous distribution of the two elements in rutile grains.

Titanite is usually a retrograded product of rutile, enriched in Nb (84–926 ppm), Ta (1.4–52 ppm) as well as other HFSEs (Zr, Hf), with Nb/Ta ranging from 12 to 61 (Table 4), which is close to, but slightly lower than, the values of rutile. No correlation between Nb and Nb/Ta was observed (Fig. 5E), likely due to limited data points.

4.3. Nb, Ta in other minerals

Niobium and Ta concentrations in garnet, omphacite, amphibole, apatite, phengite and epidote were also analyzed to better understand the behavior of these two elements during subduction. The results showed that all minerals, including garnet, omphacite, apatite, epidote and phengite, have very low Nb and Ta concentrations, mostly around detection limits (Table 5). Amphibole has also low Nb and Ta (Nb, 0.03–0.8 ppm; Ta, 0.01–0.02 ppm), but its Nb/Ta ratios are significantly fractionated (2.0 to 67, Fig. 5F).

5. Discussion

5.1. Nb–Ta fractionation by amphibole

Amphibole has higher Ti concentration than other minerals, with the exception of rutile and titanite, implying that amphibole may be the main host of Nb and Ta in the absence of Ti-bearing minerals. The Nb/Ta ratios in amphibole range from 2.0 to 67 (Table 5), falling in two groups in Nb and Ti versus Nb/Ta diagrams (Figs. 5F and 6). For eclogite with metamorphic temperatures below 900 °C, amphibole is stable at pressures of 2.5 GPa or even higher, depending on water content (Xiong et al., 2005); therefore, considerable amounts of the amphibole may have survived the UHPM. Amphibole grains with lower Nb/Ta have higher Al contents, which correspond to higher pressures. Given that low-$Mg^{\#}$ amphibole favors Nb over Ta (Ionov and Hofmann, 1995; Foley et al., 2002), the very low Nb/Ta indicates that those amphibole grains formed in an environment with very low Nb/Ta. The most likely low Nb/Ta source is fluids released at the early stage of subduction as previously proposed (Kamber and Collerson, 2000; Xiao et al., 2006). High temperature experiments show that Ti, Nb and Ta are all fluid-mobile at temperatures between 350 to 700 °C and 5 kbar (Ding et al., 2009). Amphibole formed at cooler and wetter regions during the early stage of subduction may absorb fluids released from hotter regions, inheriting the low Nb/Ta signature. Moreover, amphibole at the early stage of subduction, before rutile appears, has higher Nb and Ta, and thus has more influence on Nb–Ta fractionation.

By contrast, amphibole grains with higher Nb/Ta values have lower Al, suggesting they formed at lower pressures, most likely during retrograde metamorphism. For these amphibole grains, it is very likely that the highly fractionated Nb/Ta in amphibole was controlled by rutile and titanite (Ding et al., 2009). Rutile (TiO_2) appears at pressure above 1.5 GPa, whereas titanite ($CaTiSiO_5$) is stable at pressures below 1.5 GPa and temperature under 700 °C (Liou et al., 1998; Xiong et al., 2005). Both rutile and titanite are known to have very high Nb and Ta concentrations, but favor Ta over Nb (Tiepolo et al., 2002; Prowatke and Klemme, 2005). Therefore, amphibole formed in the presence of these two minerals tends to have low Nb, Ta concentrations with high Nb/Ta. As shown in Fig. 2C, rutile reacted with silicate minerals and partially converted to titanite in retrograded eclogite. Small amounts of Nb might have been released during this reaction, as is implied by the systematically lower Nb/Ta in

Table 4
Trace element concentrations of rutile and titanite in eclogites from CCSD (ppm).

Sample	Location [a]	Mineral[b]	Ti	V	Cr	Zr	Nb	Nb*	Hf	Ta	Ta*	U	Nb/Ta	Nb/Ta*
04303	Retrograde eclogite CCSD-MH	Rut-1	593,513	1650	59.2	115	247	286	5.14	11.9	15.2	0.300	20.8	18.8
	(193 m)	Rut-2	593,513	1761	60.3	138	256	296	5.94	12.2	15.6	4.81	21.0	19.0
		Rut-3	593,513	1879	42.2	116	247	286	5.24	12.4	15.9	1.27	20.0	18.1
		Rut-4	593,513	1744	52.1	109	247	286	4.61	11.0	14.1	3.33	22.5	20.4
		Rut-5	593,513	1623	53.8	108	237	275	5.16	11.4	14.6	1.68	20.9	18.9
		Rut-6	593,513	1826	43.3	114	286	331	3.91	11.6	14.9	0.250	24.6	22.2
04304	Retrograde eclogite CCSD-MH	Rut-1	593,513	1849	390	136	188	217	5.38	9.76	12.5	7.74	19.3	17.4
	(218 m)	Rut-2	593,513	1608	313	131.7	183.5	212.4	5.31	11.6	14.9	5.36	15.8	14.2
		Rut-3	593,513	1684	388	130	208	241	5.54	10.5	13.5	3.93	19.8	17.9
		Rut-4	593,513	1789	363	118	199	230	5.21	10.9	13.9	4.43	18.3	16.5
		Rut-5	593,513	1652	345	127	177	205	5.22	10.2	13.1	7.07	17.4	15.7
		Rut-6	593,513	1822	361	106	179	207.4	4.04	10.3	13.2	2.53	17.4	15.7
06022	Retrograde eclogite. CCSD-MH	Rut-1	593,513	1608	19.9	145	174	201	4.88	8.50	10.9	5.08	20.5	18.5
	(340 m)	Rut-2	593,513	1624	23	159	171	198	7.26	8.74	11.2	5.31	19.7	17.7
		Rut-3	593,513	1619	22	139	177	205	4.99	8.47	10.9	3.56	20.9	18.9
04307	Eclogite CCSD-MH (343 m)	Rut-1	593,513	2468	4.14	157	69.3	80.2	4.54	1.66	2.13	7.21	41.7	37.7
		Rut-2	593,513	2336	5.89	143	79.7	92.3	4.98	3.26	4.18	6.79	24.5	22.1
		Rut-3	593,513	2436	4.37	121	70.4	81.5	4.09	3.70	4.74	7.57	19.0	17.2
03558	Eclogite CCSD-MH (370 m)	Rut-1	593,513	1441	219	124	168	195	4.89	21.6	27.7	10.1	7.80	7.04
		Rut-2	593,513	1412	202	125	155	179.8	5.06	10.2	13.1	9.84	15.2	13.7
03564	Eclogite CCSD-MH (521 m)	Rut-1	593,513	1993	4.92	166	142	165	6.94	6.04	7.74	9.37	23.6	21.3
		Rut-2	593,513	1811	19.9	158	288	333	6.94	7.55	9.68	5.73	38.2	34.4
		Rut-3	593,513	2005	10.4	132	121	141	6.16	7.26	9.31	4.15	16.8	15.2
		Rut-4	593,513	2071	19.6	14.7	25.0	29.0	1.67	4.72	6.05	0.050	5.31	4.79
06018	Eclogite CCSD-MH (550 m)	Rut-1	593,513	2441	391	217	27.7	32.1	9.22	2.35	3.01	0.920	11.8	10.7
		Rut-2	593,513	2423	383	509	28.5	33.0	10.2	3.04	3.90	1.16	9.39	8.48
		Rut-3	593,513	2376	388	198	28.5	32.9	8.46	3.51	4.50	2.43	8.11	7.32
		Rut-4	593,513	2513	383	240	28.3	32.7	9.25	2.26	2.90	0.970	12.5	11.3
		Rut-5	344,717	1508	330	114	11.0	12.7	4.07	0.640	0.820	0.690	17.1	15.5
		Rut-6	593,513	2321	336	211.4	21.9	25.3	7.37	1.26	1.62	0.820	17.3	15.7
		Rut-7	593,513	2298	352	209	22.2	25.7	8.55	1.20	1.54	0.950	18.5	16.7
		Rut-8	593,513	2348	377	214	23.2	26.9	7.50	1.14	1.46	0.650	20.4	18.4
03568	Eclogite CCSD-MH (881 m)	Rut-1	593,513	585	205	7.55	49.6	57.4	0.350	5.51	7.06	0.050	9.00	8.13
		Rut-2	593,513	1209	307	4963	630	730	8.07	25.8	33.0	0.500	24.5	22.1
		Rut-3	593,513	1183	245	165	476	551	5.43	22.4	28.7	0.600	21.3	19.3
		Rut-4	593,513	1066	232	142	434	502	5.02	21.1	27.0	0.700	20.6	18.6
		Rut-5	593,513	1118	386	167	475	550	6.29	23.1	29.6	0.460	20.6	18.6
		Rut-6	593,513	1198	314	195	524	607	6.81	22.8	29.2	0.720	23.1	20.8
		Rut-7	593,513	1052	256	119	503	583	4.71	20.7	26.5	2.24	24.4	22.0
		Rut-8	593,513	1078	240	120	474	549	4.00	18.3	23.5	3.36	25.9	23.4
04313	Eclogite CCSD-MH (952 m)	Rut-1	593,513	1417	699	156	332	384	6.28	15.2	19.4	0.470	21.9	19.8
		Rut-2	593,513	1431	696	131	338	391.2	5.17	16.9	21.6	0.350	20.0	18.1
04319	Eclogite CCSD-MH (2007 m)	Rut-1	593,513	1419	512	137	212	245	6.18	8.63	11.1	0.150	24.6	22.2
		Rut-2	593,513	1369	481	146	270	313	5.16	12.1	15.5	0.070	22.4	20.2
		Rut-3	593,513	1380	503	120	254	294	6.12	11.8	15.1	0.180	21.6	19.5
		Rut-4	593,513	1385	502	150	253	293	5.32	11.5	14.8	0.040	22.0	19.9
		Rut-5	593,513	1399	632	145	239	277	7.20	10.6	13.56	0.830	22.6	20.5
		Rut-6	593,513	1405	643	147	231	267	6.61	11.7	15.1	1.12	19.7	17.8
		Rut-7	593,513	1416	575	131	236	274	6.07	13.5	17.2	0.140	17.6	15.9
		Rut-8	593,513	1470	723	171	272	315	6.18	15.2	19.5	1.19	18.0	16.2
04325[c]	Amphibolite CCSD-MH (2317 m)	Ttn-1	279,472	700	142	74.2	368	426	2.96	21.9	28.1	0.890	16.8	15.2
		Ttn -2	299,748	621	122	58.9	219	254	2.56	13.6	17.4	1.00	16.2	14.7
		Ttn -3	299,748	632	259	72.1	376	436	3.44	28.2	36.1	0.620	13.4	12.1
		Ttn -4	299,694	628	242	70.1	349	404	2.85	20.4	26.2	0.630	17.1	15.4
		Ttn -5	593,513	1336	623	144	800	926	6.11	40.4	51.8	2.18	19.8	17.9
		Ttn -6	299,694	637	196	67.6	291	337	2.74	15.1	19.3	0.660	19.4	17.5
		Ttn -7	299,694	615	81.9	52.3	72.5	83.9	1.71	1.07	1.37	1.04	67.5	61.2
		Ttn -8	299,694	598	147	69.3	375	434	2.79	18.7	24.0	1.07	20.1	18.1
4325[c]	Amphibolite CCSD-MH (2317 m)	Ttn-9	593,513	1031	492	140	618	715	4.83	30.4	38.9	1.73	20.5	18.4
		Ttn-10	593,513	944	484	127	609	705	4.51	30.1	38.6	2.50	20.3	18.3
		Ttn-11	593,513	945	418	132	614	711	5.15	31.1	39.8	1.18	19.8	17.9
04342	Eclogite CCSD-MH (2762 m)	Rut-1	593,513	957	605	154	886	1025	6.45	47.1	60.3	1.51	18.8	17.0
		Rut-2	593,513	926	621	143	895	1037	6.44	43.6	55.9	1.690	20.5	18.6
		Rut-3	593,513	731	739	142	933	1080	6.25	47.5	60.8	0.670	19.7	17.8
		Rut-4	593,513	918	590	149	884	1023	7.51	49.7	63.7	1.420	17.8	16.1
03530	Eclogite (Tuofeng outcrop)	Rut-1	593,513	2017	286	94.3	919	1064	4.3	57.9	74.2	0.080	15.9	14.4
		Rut-2	593,513	2031	302	103	886	1025	5.16	75.2	96.4	0.350	11.8	10.6
		Rut-3	593,513	1901	424	93.8	659	763	4.41	63.0	80.7	0.080	10.5	9.46
		Rut-4	593,513	1921	441	104	839	971	4.47	102	130	0.280	8.25	7.45
		Rut-5	593,513	2026	439	95.0	947	1096	4.53	49.5	63.5	0.060	19.1	17.3
		Rut-6	593,513	2005	414	96.5	969	1121	4.17	71.3	91.4	0.060	13.6	12.3
05013	Eclogite (Maobei outcrop)	Rut-1	593,513.	1885	902	119	23.2	26.8	6.11	0.700	0.900	0.130	33.4	29.9
		Rut-2	593,513	1983	790	115	22.4	25.9	5.83	0.640	0.820	0.170	34.9	31.5
		Rut-3	593,513	1787	815	141	23.4	27.1	6.46	0.820	1.05	3.430	28.6	25.8

(continued on next page)

Table 4 (*continued*)

Sample	Location [a]	Mineral[b]	Ti	V	Cr	Zr	Nb	Nb*	Hf	Ta	Ta*	U	Nb/Ta	Nb/Ta*
05013	Eclogite (Maobei outcrop)	Rut-4	593,513.	2036	856	149	25.1	29.1	7.31	0.730	0.940	4.18	34.2	31.2
		Rut-5	593,513	1935	905.	136	22.6	26.2	6.97	0.820	1.05	0.130	27.7	24.9
		Rut-6	593,513	1952	765	450	22.3	25.9	17.79	1.24	1.59	0.290	18.1	16.3
03552	Eclogite (outcrop near the main hole of CCSD)	Rut-1	593,513	2552	5.17	271	26.9	31.2	8.56	1.10	1.41	4.69	24.5	22.1
		Rut-2	593,513	2996	11.1	353	108	125	9.26	1.52	1.95	5.94	71.5	64.6
		Rut-3	593,513	3240	5.20	295	87.0	100	10.09	1.28	1.64	4.83	68.2	61.4
		Rut-4	593,513	2117	3.38	190	69.9	81.0	4.55	1.04	1.33	4.09	67.4	60.7
		Rut-5	593,513	2808	6.32	278	157	182	9.58	1.67	2.14	4.63	94.5	85.4
		Rut-6	593,513	2835	6.79	260	146.	169	9.11	1.72	2.20	5.14	84.9	76.7
		Rut-7	593,513	2870	4.13	362	33.1	38.3	10.8	1.09	1.40	11.0	30.4	27.4
		Rut-8	593,513	2926	4.74	244	31.7	36.7	7.15	1.16	1.49	2.74	27.2	24.6
		Rut-9	593,513	2813	5.06	311	148	171	9.43	1.54	1.97	4.78	96.2	86.9
		Rut-10	593,513	2633	4.11	268	108	125	9.07	1.24	1.59	4.68	87.5	78.7
		Rut-11	593,513	2741	4.50	276	94.9	109	9.22	1.32	1.69	4.83	72.0	64.9
		Rut-12	593,513	2930	4.18	239	37.1	43.0	7.59	0.980	1.26	2.60	37.9	34.2
B154	Eclogite (pilot hole of CCSD)	Rut-1	593,513	3064	3.43	169	16.9	19.6	6.27	1.37	1.76	2.71	12.3	11.2
		Rut-2	593,513	2908	4.22	166	17.6	20.3	5.72	1.32	1.69	3.02	13.3	12.0
		Rut-3	593,513	3110	4.02	151	19.4	22.4	6.23	1.24	1.59	2.8	15.6	14.1
		Rut-4	593,513	3082	4.90	152	16.7	19.4	4.79	1.36	1.74	2.52	12.3	11.1
		Rut-5	593,513	3094	6.67	180	16.4	19.0	7.01	0.950	1.22	2.51	17.2	15.6
		Rut-6	593,513	2601	4.00	164	16.5	19.2	6.55	1.03	1.32	2.76	16.1	14.5
05016	Eclogite (Qinglongshan outcrop)	Rut-1	593,513	31,555	3840	28.9	7.24	8.38	29.53	0.16	0.210	0.180	45.3	40.8
		Rut-2	593,513	33,037	4290	25.6	16.2	18.7	0.870	0.570	0.730	0.120	28.4	25.6
		Rut-3	593,513	33,280	3595	20.2	26.3	30.4	0.850	0.290	0.370	0.280	90.7	81.9
05022	Eclogite (Qinglongshan outcrop)	Rut-1	593,513	918	433	118	286	331.9	4.10	12.4	15.9	0.040	23.2	20.9
		Rut-2	593,513	869	413	114	284	329.3	4.68	10.4	13.3	0.030	27.5	24.8
		Rut-3	593,513	13,377	5594	18.9	38.0	44.0	52.17	0.640	0.820	10.0	59.6	53.6
		Rut-4	593,513	12,131	6531	29.4	52.8	61.1	1.41	1.58	2.03	1.59	33.4	30.2
03550	Eclogite (Sanqingge outcrop)	Rut-1	593,513	1481	108	161	155	180	5.23	8.51	10.9	7.59	18.3	16.5
		Rut-2	593,513	1539	115	158	162	188	5.38	8.22	10.5	9.49	19.8	17.9
		Rut-3	593,513	1502	92.5	147	130	150	4.43	6.12	7.85	13.2	21.3	19.2
		Rut-4	593,513	1497	86.0	137	125	145	3.97	6.60	8.46	12.6	19.0	17.1
		Rut-5	593,513	1509	88.1	136	128	148	3.57	6.83	8.76	10.1	18.8	17.0
		Rut-6	593,513	1563	102	155	147	171	4.71	8.86	11.4	12.3	16.7	15.1
		Rut-7	593,513	1521	98.8	157	148	172	5.79	9.32	12.0	11.0	16.0	14.4
		Rut-8	593,513	1529	97.5	148	145	168	5.04	8.50	10.9	9.96	17.1	15.5
		Rut-9	593,513	1536	96.8	150	152	175	4.41	10.6	13.5	10.4	14.4	13.0
		Rut-10	593,513	1533	87.1	131	129	150	3.54	6.81	8.73	11.5	19.1	17.2
		Rut-11	593,513	1533	85.7	123	125	145	3.54	6.51	8.35	9.40	19.3	17.4
		Rut-12	593,513	1537	88.4	488	131	152	3.94	6.92	8.87	12.7	19.0	17.2
		Rut-13	593,513	1524	98.0	148	142	165	4.55	7.09	9.09	9.44	20.2	18.2

Trace element concentrations in ppm, the values of Nb/Ta, (Nb/Ta)* in percentage.
[a]CCSD-M.H. – the main hole of CCSD; [b] Rut – rutile, Ttn – titanite; [c] the amphibolite is the retrograde product of eclogite, see the details in the text.
*Modified concentrations of Nb, Ta and the ratios of Nb/Ta according to the suggested values of Nb and Ta of the external standard NIST 610 by Hu et al. (2008).

titanite. These observations explain the high Nb/Ta in low pressure amphibole.

Additionally, previous experiments show that $^{Amph/L}D_{Nb/Ta}$ for low-Mg# amphibole formed in subduction setting is up to 1.6, considerably higher than high-Mg# amphibole (Tiepolo et al., 2000). Therefore, eclogitic amphibole, which usually has low Mg# [Mg/(Mg + Fe)], favors Nb over Ta (Oberti et al., 2000; Tiepolo et al., 2000, 2001; Foley et al., 2002). Fluids released during blueschist-to-amphibolite transformation should have much lower Nb/Ta ratios than the protolith (Xiao et al., 2006). Amphibole from CCSD drill holes has low Mg# (0.52–0.55) and Ti (821–3650 ppm) (Xiao et al., 2006), which belongs to low-Mg# amphibole (Mg# < 0.70) (Tiepolo et al., 2000; Foley et al., 2002).

Note that the amphiboles in this study have much lower Nb and Ta compared to published data (Ionov and Hofmann, 1995). This is probably because of the different formation environment and mineral assemblage. For example, amphibole in eclogites is commonly associated with rutile, titanite, or a combination of both. By contrast, amphibole from peridotite coexists with olivine and pyroxene.

5.2. Rutile in subduction zone

Rutile is strongly enriched in Nb, Ta and Ti compared to other HFSEs, which are depleted in other minerals in eclogite, i.e., most of Nb and Ta in eclogite are hosted by rutile, such that rutile dominates the whole rock Nb, Ta budget, so the whole rock Nb/Ta of eclogite should be close to that of rutile (Rudnick et al., 2000). This is consistent with previous studies on eclogites (Zack et al., 2002) and metasomatised peridotite xenoliths (Kalfoun et al., 2002), showing that more than 90% of Nb and Ta are hosted in rutile. To verify the role of rutile hosting Nb and Ta in the whole rock, we selected two fresh eclogites to calculate the contribution of rutile to the whole rock for HFSEs. The result indicates that more than 90% of Nb, Ta and Ti are controlled by rutile (Table 6. Fig. 7).

Interestingly, the Nb/Ta of whole rocks range from 8.7 to 24.5 (Table 2), which is less varied than rutile grains. This seems to contradict the assertion that rutile hosts more than 90% of the Nb, Ta in eclogites, but the most likely reason is that eclogite samples usually have rutile grains formed at different stages with different Nb/Ta. In addition, Nb and Ta are also heterogeneous within single rutile grains (i.e., Ti is not correlated with Nb, Ta even in rutile). Moreover, rutile grains in CCSD samples are usually very large, so drill hole samples are usually too small to get representative results for elements hosted by large minerals. This also explains the lack of correlation between Nb/Ta and Ti (Fig. 3C).

Decoupling between Ti and Nb (and Ta), described by previous authors (Liu et al., 2008), is not observed. Most of the samples studied by Liu et al. (2008) were from the ilmenite-enriched layer (Zhang et al., 2004; Liu et al., 2008). In general, ilmenite has much lower Nb, Ta compare to rutile (Ding et al., 2009), such that it weakened the correlation between Nb, Ta and Ti.

Table 5
Concentrations of trace elements in minerals of eclogites from CCSD (ppm).

Sample	Location [a]	Mineral [b]	Ti	V	Cr	Zr	Nb	Hf	Ta	U	Nb/Ta [c]
03552	Near the main hole	Grt(c)	411	248	3.01	2.33	0.034	<0.053	<0.010	<0.013	–
		Grt(r)	492	260	3.67	4.6	0.037	<0.086	<0.009	0.055	–
04307	343m	Grt(inc1)	239	115	32.3	0.553	<0.023	<0.057	<0.006	<0.014	–
		Grt(inc2)	188	119	43.8	0.509	0.04	<0.044	<0.009	0.01	–
		Grt(inc3)	279	87.2	230	1.24	<0.027	<0.100	<0.009	<0.028	–
04305	235m	Grt(c)	279	90.8	8.59	1.12	<0.026	<0.074	<0.003	<0.018	–
		Grt(r)	208	70.3	7.04	1.01	0.028	<0.051	<0.007	<0.019	–
04314	1082m	Grt(c)	73.3	24.8	52.6	0.88	0.033	<0.043	<0.005	0.006	–
		Grt(r)	61.5	24.3	59.5	1.07	0.029	<0.057	0.01	0.016	–
04336	2710m	Grt(c)	208	65.3	125	1.53	<0.022	<0.067	<0.007	<0.015	–
03552	Near the main hole	Omp(c)	431	881	2.46	7.21	<0.016	0.132	<0.005	<0.008	–
		Omp(r)	434	881	2.97	2.79	<0.024	0.188	<0.008	0.003	–
04307	343m	Omp(c)	460	726	7.16	2.8	<0.020	0.179	<0.004	<0.014	–
		Omp(r)	442	722	6.33	2.4	<0.013	0.139	<0.004	0.012	–
04305	235m	Omp(c)	436	443	18.7	1.02	<0.014	<0.073	<0.006	0.008	–
		Omp(r)	434	445	15.4	1.01	<0.012	<0.065	<0.002	0.006	–
		Omp(c)	322	326	175	1.84	<0.019	0.151	<0.003	<0.006	–
		Omp(r)	351	317	124	1.96	<0.012	0.124	<0.003	<0.01	–
03564	521m	Omp(inc)	457	1025	30.1	1.88	0.03	0.152	<0.006	<0.012	–
04336	2710m	Ap(inc)	3.23	0.718	4.82	<0.065	<0.013	<0.030	<0.006	1.65	–
04307	343m	Ap(c)	<0.380	0.767	<0.910	<0.055	<0.015	<0.025	<0.006	5.15	–
		Ap(r)	<0.27	0.872	2.34	<0.081	<0.016	<0.030	<0.001	3.79	–
		Ap(inc)	249	3.88	3.54	0.14	0.059	<0.019	<0.002	8.83	–
04311	544m	Ap(c)	1.84	0.432	12.2	<0.068	<0.003	<0.008	<0.001	0.457	–
		Ap(r)	5.65	0.686	6.21	<0.058	<0.005	<0.02	<0.002	0.183	–
		Ap(c)	<0.180	0.167	39.4	<0.050	<0.008	<0.019	<0.001	15.5	–
04301	163m	Phn(c)	2308	303	118	0.123	0.31	<0.013	<0.004	0.181	–
		Phn(r)	1928	295	114	0.113	0.307	<0.064	<0.011	0.225	–
		Phn(r)	9142	487	132	0.482	0.26	<0.041	<0.009	0.018	–
03558A	370m	Phn(c)	2737	389	149	0.181	0.132	<0.042	0.015	0.021	8.6
		Phn(r)	1138	449	123	2.32	0.062	<0.090	<0.003	0.015	–
04309	449m	Phn(inc)	734	52.1	182	0.722	<0.024	<0.031	<0.005	<0.010	–
04313	952m	Phn(inc)	1879	372	361	0.18	0.064	<0.034	<0.007	<0.007	–
		Phn(c)	1894	464	248	0.354	0.062	<0.035	0.017	0.024	3.6
04318	1939m	Phn(c)	1809	301	508	<0.079	0.142	<0.015	0.015	<0.005	9.1
04314	1082m	Epi(c)	307	239	100	3.36	0.029	0.125	<0.008	60.8	–
04336	2710m	Epi(c)	2372	185	80.6	34.2	0.036	0.95	0.012	0.1	3
		Epi(r)	1557	241	146	15.6	0.062	0.29	<0.007	0.121	–
05043	3054m	Epi(c)	834	282	75.4	15.6	0.037	0.33	<0.009	<0.022	–
		Aln(c)	520	319	53	2.05	<0.019	<0.072	<0.005	482	–
		Epi(r)	602	330	56.5	6.52	0.031	0.274	<0.007	6.01	–
03537	Qinglong-shan	Epi(c)	365	324	130	4.35	<0.012	0.2	<0.002	0.799	–
		Epi(r)	420	386	80.5	5.55	<0.008	0.213	<0.002	0.551	–
04332	2681m	Aln(c)	723	45.7	5.4	3.14	<0.012	0.159	<0.004	207	–
		Epi(r)	846	73.5	5.19	10.3	<0.012	0.42	<0.003	3.04	–
04320	2033m	Amp1-1	1613	292	174	3.66	0.051	0.269	0.011	<0.012	4.68
		-2	2661	423	316	3.05	0.066	0.164	0.011	<0.014	6.23
		-3	3186	322	154	4.48	0.095	0.259	0.017	<0.012	5.46
		Amp2-1	3197	256	100	3.71	0.083	0.267	0.01	<0.012	7.98
		-2	1805	231	128	2.9	0.193	<0.105	0.015	<0.018	13
		-3	2559	201	208	3.23	0.186	0.153	0.013	<0.012	13.9
		Amp3-1	2008	206	5.4	4.04	0.163	0.188	0.016	0.018	10
		-2	102	90.5	96.1	4.37	<0.022	0.152	0.011	0.027	–
		-3	221	110	40.9	2.93	<0.02	<0.081	0.011	0.02	–
04325	2317m	Amp1-1	2825	325	133	5.91	0.699	0.243	0.012	<0.012	58.7
		-2	3346	337	200	5.15	0.601	0.301	0.011	<0.013	52.7
		Amp2-1	3200	333	296	5.5	0.812	0.283	0.016	<0.014	52.4
		-2	3212	305	130	5.99	0.756	0.233	<0.009	<0.012	–
		-3	3106	342	177	5.82	0.733	0.127	0.013	<0.011	56.4
		Amp3-1	2922	386	202	3.88	0.55	0.28	0.013	<0.011	42.6
		-2	2717	390	153	5.3	0.754	0.183	0.011	<0.009	67.3
		Amp4-1	2276	306	183	3.47	0.518	0.123	0.011	<0.010	48.4
		-2	206	24.9	30.7	0.454	0.031	<0.104	0.015	<0.013	2.03
B691	1255m	Amp1-1	685	282	172	2.32	0.088	0.21	0.02	<0.020	4.51
		-2	1705	336	132	5.7	0.506	0.38	0.013	<0.016	37.8
		Amp2-1	3054	295	133	8.88	0.451	0.406	0.011	<0.010	42.9
		-2	2434	344	280	5.87	0.714	0.334	0.019	<0.016	38

[a] The number with unit as meter is the depth of the main hole of CCSD.
[b] Gar – garnet, Omp – omphacite, Ap – apatite, Phn – phengite, Epi – epidote, Aln – allanite, Amp – amphibole, r – rim, c – core, inc – inclusion.
[c] – Not calculated Nb/Ta for those which concentration of Nb or Ta or both of them are below detection limits.

The significance of rutile in subduction zones in terms of Nb, Ta behaviors has long been recognized (e.g., McDonough, 1991; Green, 1995). The well-known negative anomalies of Ti, Nb and Ta in the continental crust and arc volcanic rocks have been attributed to the presence of rutile in the source region (e.g., McDonough, 1991). Partial melting experiments using a starting material of natural basalt

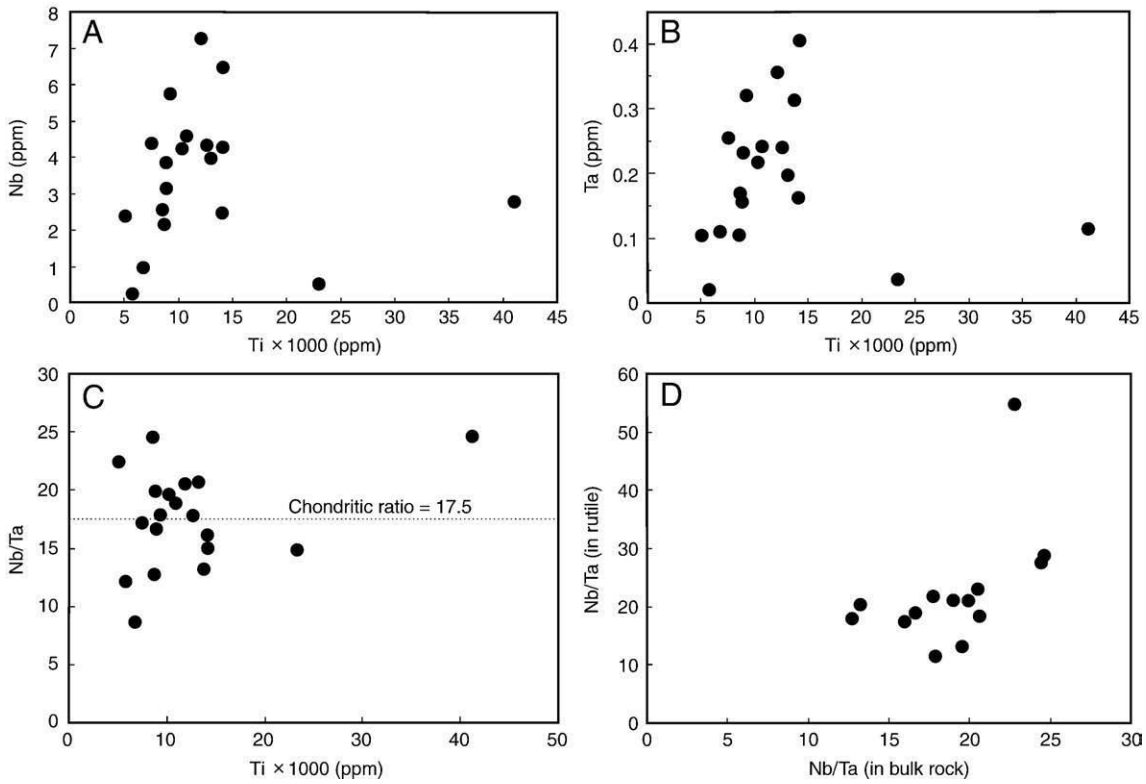

Fig. 3. Diagrams of Nb, Ta and Nb/Ta versus Ti in bulk rocks, and Nb/Ta in rutile versus Nb/Ta in bulk rocks. Nb and Ta are weakly positive correlated with Ti. The lack of correlation between Ti and Nb, Ta was used to argue against the generally accepted idea that rutile controls Nb and Ta budget in eclogites (Liu et al., 2008). For the CCSD samples, Nb and Ta are not homogenous (not correlated with Ti) in rutile, therefore the argument is not sound.

(with 2 to 5 wt.% H_2O added) at 1.0–2.5 GPa and 900–1100 ºC show that rutile is a necessary residual phase during generation of melt with compositions similar to Archean TTG magmas (or adakite in modern arc island setting) (Rapp et al., 1991; Xiong et al., 2005; Xiong et al., 2006). Therefore, rutile is a good indicator to trace the formation and evolution of the continental crust (Brenan et al., 1994; Barth et al., 2000; Munker et al., 2004; Klemme et al., 2005b; Xiao et al., 2006; Xiong et al., 2006).

Experimental results, however, show that rutile favors Ta over Nb, such that partial melting of subducting slabs in the presence of rutile should produce melt with higher Nb/Ta (Foley et al., 2000; Horng and Hess, 2000; Foley et al., 2002; Schmidt et al., 2004; Klemme et al., 2005a; Xiong et al., 2005; Bromiley and Reffern, 2008; Klimm et al., 2008). The structural characteristics of edge-sharing TiO_2 octahedra make rutile offer only one crystal site around 0.58 Å in size, which is smaller than all the main trace elements; Nb and Ta are closest to the size and thus have the highest rutile/melt partition coefficients (Foley, 2008). The ionic radii of Nb is actually slightly larger than that of Ta (Tiepolo et al., 2000), thus Ta is more compatible in rutile than Nb. This means that partial melting of subducting slabs that contain rutile is unlikely to produce lower Nb/Ta ratios in melt than the starting material in the presence of rutile. The Nb/Ta value of the

Table 6
Contributions of each mineral to bulk rock for HFSEs.

Mineral	Modes (%)	Zr (%)	Nb (%)	Hf (%)	Ta (%)	Ti (%)
Sample: 04308						
Ap	1.00	0.090	0.010	0.440	0.110	0.000
Epi	1.80	1.48	0.020	1.79	0.100	0.120
Aln	1.23	0.540	0.010	0.670	0.050	0.130
Phn	1.53	0.090	0.160	0.340	0.150	0.610
Rt	0.940	27.5	98.7	30.4	94.9	94.4
Omp	40.0	57.4	0.270	52.3	0.960	2.45
Grt	53.5	12.9	0.840	14.0	3.72	2.31
Sample: 03558						
Ap	0.85	0.70	0.030	1.26	0.160	0.000
Phn	1.74	0.61	0.070	0.700	0.100	0.390
Rt	1.41	62.17	98.6	51.2	93.7	95.8
Omp	45.00	20.18	0.550	33.2	2.79	1.94
Grt	51.00	16.35	0.730	13.6	3.28	1.88

Note:
The mineral modal abundance was determined based on thin-section observation and point counting on the sections. The modal abundance of rutile was calculated assuming that it is the main host of Ti in the bulk rock; The contributions of each mineral to bulk rock for HFSEs was calculated using average mineral trace elements concentration for each element and the corresponding modal abundance of each mineral. Ap – apatite; Epi – epidote; Aln – allanite; Phn – phengite; Rt– rutile; Omp – omphacite; Grt – garnet.

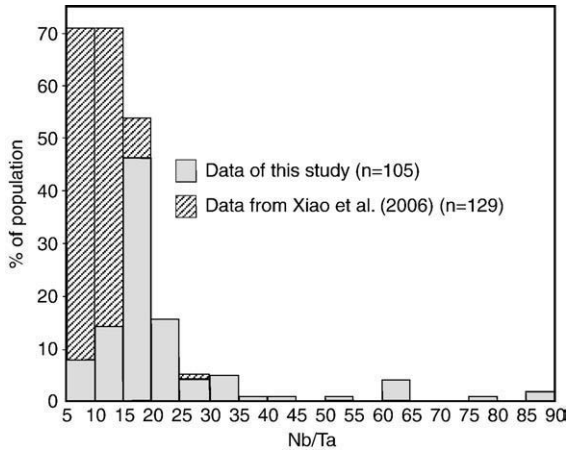

Fig. 4. Histogram of Nb/Ta ratios in rutile from CCSD samples. Also shown are data from Xiao et al. (2006) for rutile grains from a pilot drill hole at depths of 180 m. Our results are much more varied with an overall suprachondritic average. This strongly suggests that Nb and Ta are mobile, likely at the early stage of plate subduction before rutile appears. The overall suprachondritic Nb/Ta supports that subducted oceanic crusts stored in the lower mantle can serve as the missing reservoir of Nb.

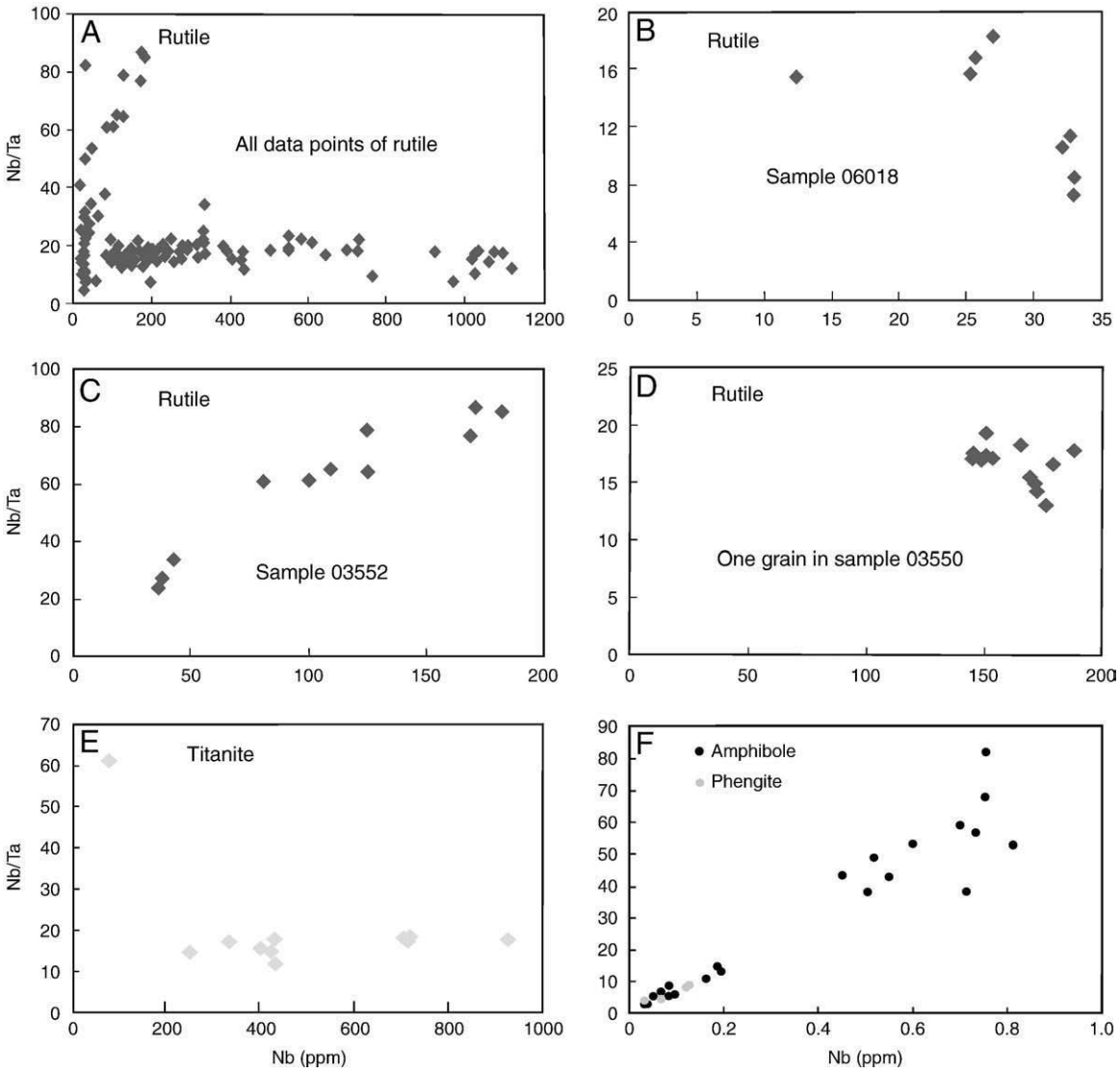

Fig. 5. Diagrams of Nb versus Nb/Ta ratios of rutile, titanite, amphibole and phengite in eclogite from CCSD, showing large fractionation between Nb and Ta.

continental crust is about 12–13 (Barth et al., 2000), whereas the average value of Nb/Ta ratios of MORB from the Atlantic, Indian and Pacific oceans are 16.7 ± 1.8 (Kamber and Collerson, 2000). Given that rutile favors Ta over Nb, partial melting of subducted oceanic slabs in the presence of rutile should form melts with suprachondritic Nb/Ta (Foley et al., 2002). For these reasons, partial melting of amphibolite in the absence of rutile has been proposed to explain the low Nb/Ta in the continental crust (Foley et al., 2002). This model, however, cannot explain the negative Nb, Ta anomalies of continental crust and arc magmas. Alternatively, partial melting of subducted slabs in the presence of rutile requires Nb, Ta fractionation beforehand (Rapp et al., 2003; Xiong et al., 2005).

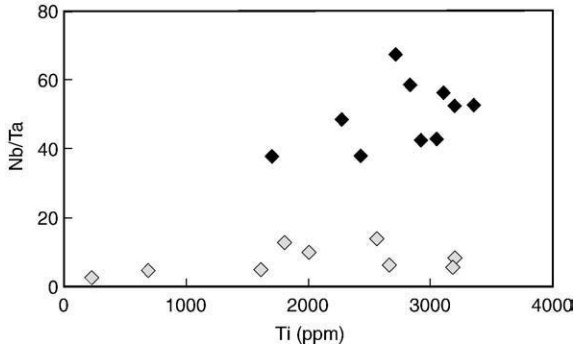

Fig. 6. The relationship between Ti concentration and Nb/Ta ratios in amphibole. Amphibole can be classified into two groups according to Nb/Ta: the group with higher Nb/Ta (dark diamonds) have higher Al contents, which correspond to higher pressures; by contrast, the lower Nb/Ta group (grey diamonds) has lower Al, suggesting they formed at lower pressures, most likely during retrograde metamorphism.

Based on highly fractionated Nb/Ta in rutile grains from a CCSD pilot drill hole, researchers have proposed a "zone refining dehydration" model to reconcile the different lines of observations (Xiao et al., 2006). The model suggests that the subducting slab may have a "sandwiched" structure, with colder regions bounded by hotter layers on both sides. In the hotter parts of the slab, major dehydration occurs during blueschist-to-amphibole eclogite transformation (BAT) that takes place in the absence of rutile (<1.5 GPa). In this case, Nb and Ta budgets are controlled by the partitioning between fluids and amphibole, and the BAT fractionates Nb from Ta, resulting in subchondritic and suprachondritic Nb/Ta in the released fluids and residual amphibole eclogites, respectively (Xiao et al., 2006). According to the zone refining model, the dehydration process results in subchondritic Nb/Ta values in the colder and wetter regions, with complementary suprachondritic Nb/Ta in the hotter and dryer

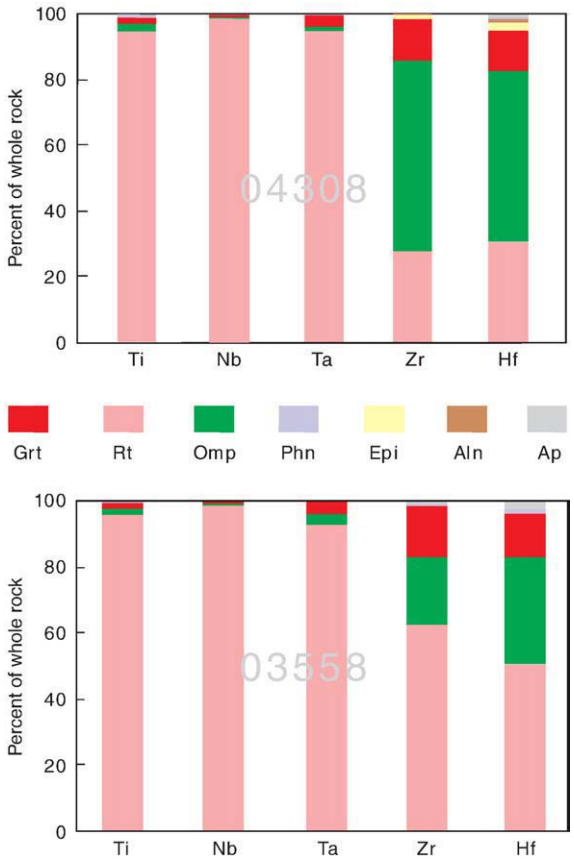

Fig. 7. Estimated HFSE budget in two fresh eclogites. Rutile controls Nb and Ta budgets.

regions of the slabs. Subsequent slab subducting results in partial melting of wetter and colder regions with subchondritic Nb/Ta (mainly controlled by H_2O contents); in contrast, the dry region (early dehydrated inner portions) with suprachondritic Nb/Ta ratios cannot be melted (Xiao et al., 2006). Hence, the fractionated Nb/Ta ratios of the subducting slabs can be transferred to the continental crust through slab melting, and the residual eclogitic phase hosts variable Nb/Ta from subchondritic to suprachondritic (Xiao et al., 2006). This model is strongly supported by our results: highly variable Nb/Ta along the CCSD drill hole with overall higher Nb/Ta at greater depths than 200 m (Fig. 8), coupled with varied but overall subchondritic Nb/Ta at shallower depths.

5.3. A hidden suprachondritic reservoir

Previous studies show subchondritic Nb/Ta values for all reservoirs of the silicate Earth sampled so far; this is known as the terrestrial Nb–Ta paradox (Barth et al., 2000; Rudnick et al., 2000; Munker et al., 2004). McDonough (1991) proposed that refractory eclogite, the residue of partially melted subducting slabs, may satisfy the mass balance requirements for Ti, Nb and Ta in the silicate Earth. This model is supported by suprachondritic Nb/Ta of rutiles in eclogitic xenoliths from African and Siberia cratonic kimberlites (Rudnick et al., 2000). It was estimated that an eclogitic reservoir accounting for about 0.5–6% of the mass of the mantle would make the mass balance in terms of Nb and Ta (Barth et al., 2000; Rudnick et al., 2000). This was challenged by partial melting experimental results, which suggests that rutile favors Ta over Nb (Foley et al., 2000; Horng and Hess, 2000; Foley et al., 2002; Schmidt et al., 2004; Klemme et al., 2005a; Xiong et al., 2005; Bromiley and Reffern, 2008; Klimm et al., 2008), and therefore, residual eclogites should have Nb/Ta lower than the starting material. Our results indicate significant Nb/Ta fractionation in the eclogites from CCSD, which occur most likely during dehydration in the absence of rutile (Xiao et al., 2006): fluids tend to have lower Nb/Ta, so the residue eclogites should have suprachondritic Nb/Ta, which could be the missing suprachondritic Nb/Ta reservoir.

5.4. The mechanism of Nb and Ta fractionation

It is generally accepted that Nb/Ta fractionation is controlled by minerals and fluids (Brenan et al., 1994; Henry et al., 1996; Stalder

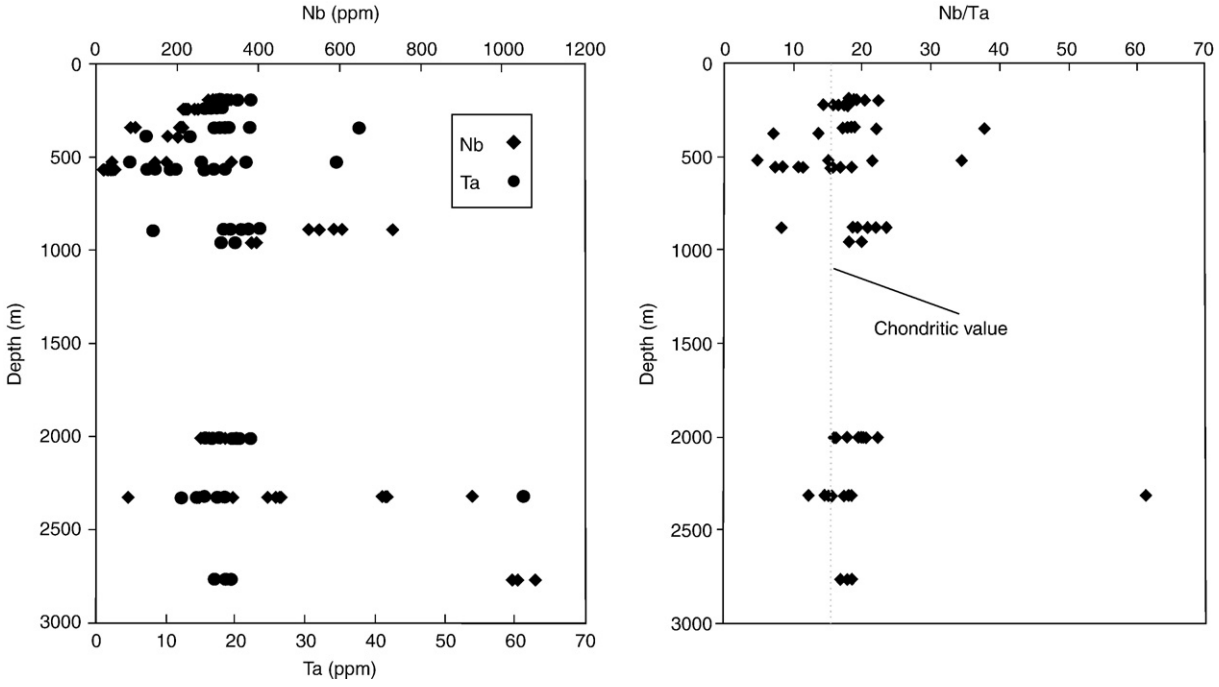

Fig. 8. Variation of Nb and Ta concentrations and Nb/Ta ratios in rutile with depths along the main hole of the CCSD. Both concentrations and Nb/Ta are highly varied.

et al., 1998; Xiao et al., 2006). Minerals with non-chondritic Nb/Ta values may have contributed to Nb/Ta fractionation. Rutile, titanite and amphibole have highly varied Nb/Ta (Fig. 5). Rutile and titanite have very high Nb, Ta concentrations, and thus would dominate the whole rock Nb and Ta budget, and be unable to fractionate the two elements effectively. Therefore, the highly fractionated Nb/Ta in rutile and titanite should be inherited from other systems. Amphibole and mica were proposed to be important hosts for Nb and Ta in the absence of rutile (Ionov and Hofmann, 1995; Ionov et al., 1999; Green and Adam, 2003; Xiao et al., 2006). Our results show that mica in eclogites has too low Nb and Ta to dramatically fractionate Nb/Ta. The reasonably high Nb and Ta concentrations coupled with varied Nb/Ta, indicate that amphibole can effectively fractionate Nb from Ta. Amphibole has the main influence on Nb/Ta fractionation (Foley et al., 2002) in the "zone refining" dehydration model (Xiao et al., 2006). The Nb and Ta concentrations in amphibole in this study are very low (Table 5), because these amphibole grains were formed during retrograde metamorphism, in the presence of rutile (Fig. 2E). It is likely that minerals with higher Ti concentrations have more influence on the behavior of Nb and Ta, due to the similar radii and valence of Nb, Ta and Ti (Horng and Hess, 2000; Schmidt et al., 2004).

6. Conclusions

Our new data set of Nb and Ta concentrations in minerals of eclogites from CCSD provides constraints on the fractionation between Nb and Ta during plate subduction, which is helpful for further understanding of the terrestrial Nb–Ta paradox.

(1) Nb fractionates from Ta significantly in eclogite and rutile. The Nb/Ta ratio varies more dramatically in rutile grains than in the bulk rock, possibly due to the inhomogeneous distribution of Nb and Ta in rutile and mixing of rutile grains of different generations in the whole rock.
(2) Amphibole is important in fractionating Nb from Ta during dehydration at the early stage of subduction in the absence of rutile.
(3) Rutile plays a significant role on the budget of HFSEs, especially, Nb, Ta and Ti in the subduction zone, because it hosts most of these elements. It is, however, not a main factor in fractionating Nb from Ta, but its high capability of hosting Nb, Ta and Ti makes it the "recorder" of the fractionation between Nb and Ta.
(4) Overall, most eclogites in this paper display superchondritic features, which supports the theory of subducted slabs as suprachondritic Nb/Ta reservoirs in the mantle.
(5) Nb, Ta fractionation during the early stage of subduction is essential in shaping the geochemical features of the continental crust.

Acknowledgments

This work was supported jointly by the National Science Foundation of China (40399142, 40525010) and the National Basic Research Program of China (973 Program) (2003C13716501). We thank Dr. Zhao Wen-xia and Ms. Chen Lin-li for their help with the electron microprobe; Dr. Liu Xiao-ming and Ms. Zhang Hong of the State Key Laboratory of Continental Dynamics of Northwest University for their help with the trace elements analysis of minerals by LA-ICP-MS; and Ms Liu Ying of CAS Key Laboratory of Isotope Geochronology and Geochemistry, Guangzhou Institute of Geochemistry for her help with the major and trace elements analysis of the whole eclogites by XRF and LA-ICP-MS. Thanks also to CCSD base for providing samples. Professor Sun-Lin Chung and Ms Elaine Chang are thanked for helping us with the English writing. Valuable review comments by Steve Foley and Balz Kamber and constructive suggestions by Roberta Rudnick are highly appreciated. This is contribution No. IS-1109 from GIGCAS.

References

Ames, L., Zhou, G.Z., Xiong, B.C., 1996. Geochronology and isotopic character of ultrahigh-pressure metamorphism with implications for collision of the Sino-Korean and Yangtze cratons, central China. Tectonics 15 (2), 472–489.
Barth, M.G., McDonough, W.F., Rudnick, R.L., 2000. Tracking the budget of Nb and Ta in the continental crust. Chemical Geology 165 (3–4), 197–213.
Brenan, J.M., Shaw, H.F., Phinney, D.L., Ryerson, F.J., 1994. Rutile-aqueous fluid partitioning of Nb, Ta, Hf, Zr, U and Th: implications for high field strength element depletions in island arc basalts. Earth and Planetary Science Letters 128 (3–4), 327–339.
Bromiley, G.D., Reffern, S.A.T., 2008. The role of TiO_2 phases during melting of subduction-modified crust: implications for deep mantle melting. Earth and Planetary Science Letters 267 (1–2), 301–308.
Chen, J., Xu, Z.Q., Li, X.P., 2005. The formation of nanometer twins of rutile and its textural characteristics in UHP eclogite. Acta Petrologica Sinica 21 (2), 399–404.
Ding, X., Lundstrom, C., Huang, F., Li, J., Zhang, Z.M., Sun, X.M., Liang, J.L., Sun, W.D., 2009. Natural and experimental constraints on formation of the continental crust based on niobium–tantalum fractionation. International Geology Review 51 (6), 473–501.
Foley, S., 2008. A trace element perspective on Archean crust formation and on the presence or absence of Archean subduction. The Geological Society of America Special Paper 440, 31–50.
Foley, S.F., Barth, M.G., Jenner, G.A., 2000. Rutile/melt partition coefficients for trace elements and an assessment of the influence of rutile on the trace element characteristics of subduction zone magmas. Geochimica Et Cosmochimica Acta 64 (5), 933–938.
Foley, S., Tiepolo, M., Vannucci, R., 2002. Growth of early continental crust controlled by melting of amphibolite in subduction zones. Nature 417 (6891), 837–840.
Green, T.H., 1995. Significance of Nb/Ta as an indicator of geochemical processes in the crust–mantle system. Chemical Geology 120 (3–4), 347–359.
Green, T.H., Adam, J., 2003. Experimentally-determined trace element characteristics of aqueous fluid from partially dehydrated mafic oceanic crust at 3.0 GPa, 650–700 degrees C. European Journal of Mineralogy 15 (5), 815–830.
Henry, C., Burkhard, M., Goffe, B., 1996. Evolution of synmetamorphic veins and their wallrocks through a western Alps transect: no evidence for large-scale fluid flow. Stable isotope, major- and trace-element systematics. Chemical Geology 127 (1–3), 81–109.
Horng, W.S., Hess, P.C., 2000. Partition coefficients of Nb and Ta between rutile and anhydrous haplogranite melts. Contributions to Mineralogy and Petrology 138 (2), 176–185.
Hu, Z.C., Gao, S., Liu, Y.S., Xu, J., Hu, S.H., Chen, H.H., 2008. Niobium and tantalum concentrations in NIST SRM 610 revisited. Geostandards and Geoanalytical Research 32 (3), 347–360.
Ionov, D.A., Hofmann, A.W., 1995. Nb–Ta-rich mantle amphiboles and micas – implications for subduction-related metasomatic trace-element fractionations. Earth and Planetary Science Letters 131 (3–4), 341–356.
Ionov, D.A., Gregoire, M., Prikhod'ko, V.S., 1999. Feldspar–Ti-oxide metasomatism in off-cratonic continental and oceanic upper mantle. Earth and Planetary Science Letters 165 (1), 37–44.
Jochum, K.P., Seufert, H.M., Spettel, B., Palme, H., 1986. The solar system abundances of Nb, Ta and Y and the relative abundances of refractory lithophile elements in differentiated planetary bodies. Geochim Cosmochim Acta 50, 1173–1183.
Jochum, K.P., McDonough, W.F., Palme, H., Spettel, B., 1989. Compositional constraints on the continental lithospheric mantle from trace elements in spinel peridotite xenoliths. Nature 340, 548.
Jochum, K.P., Stoll, B., Herwig, K., et al., 2006. MPI-DING reference glasses for in situ microanalysis: new reference values for element concentrations and isotope ratios. Geochemistry, Geophysics, Geosystems 7, Q02008. doi:10.1029/2005GC001060.
Kalfoun, F., Ionov, D., Merlet, C., 2002. HFSE residence and Nb/Ta ratios in metasomatised, rutile-bearing mantle peridotites. Earth and Planetary Science Letters 199 (1–2), 49–65.
Kamber, B.S., Collerson, K.D., 2000. Role of 'hidden' deeply subducted slabs in mantle depletion. Chemical Geology 166 (3–4), 241–254.
Kamber, B.S., Greig, A., Schoenberg, R., Collerson, K.D., 2003. A refined solution to Earth's hidden niobium: implications for evolution of continental crust and mode of core formation. Precambrian Research 126 (3–4), 289–308.
Klemme, S., Prowatke, S., Hametner, K., Gunther, D., 2005a. Partitioning of trace elements between rutile and silicate melts: implications for subduction zones. Geochimica Et Cosmochimica Acta 69 (9), 2361–2371.
Klemme, S., Prowatke, S., Hametner, K., Gunther, D., 2005b. Trace element partitioning between rutile and melt with implications for element transfer in subduction zones. Geochimica Et Cosmochimica Acta 69 (10), A661-A661.
Klimm, K., Blundy, J.D., Green, T.H., 2008. Trace element partitioning and accessory phase saturation during H_2O-saturated melting of basalt with implications for subduction zone chemical fluxes. Journal of Petrology 49 (3), 523–553.
Li, S.G., Jagoutz, E., Chen, Y.Z., Li, Q.L., 2000. Sm–Nd and Rb–Sr isotopic chronology and cooling history of ultrahigh pressure metamorphic rocks and their country rocks at Shuanghe in the Dabie Mountains, Central China. Geochimica Et Cosmochimica Acta 64 (6), 1077–1093.
Liang, J.L., Sun, X.M., Xu, L., Zhai, W., Tang, Q., Liang, Y.H., 2006. Geochemistry of epidotes in HP–UHP metamorphic rocks from Chinese Continental Scientific Drilling (CCSD) Project and Qinglongshan area: an indicator of partial melting during continental slab exhumation. Acta Petrologica Sinica 22 (7), 1845–1854.
Liou, J.G., Zhang, R.Y., Ernst, W.G., Liu, J., McLimans, R., 1998. Mineral parageneses in the Piampaludo eclogitic body, Gruppo di Voltri, Western Ligurian Alps. Schweizerische Mineralogische Und Petrographische Mitteilungen 78 (2), 317–335.

Liu, X.M., Gao, S., Yuan, H.L., Hattendorf, B., Gunther, D., Chen, L., Hu, S.H., 2002. Analysis of 42 major and trace elements in glass standard reference materials by 193 nm LA-ICPMS. Acta Petrologica Sinica 18 (3), 408–418.
Liu, F.L., Xu, Z.Q., Xue, H.M., 2004. Tracing the protolith, UHP metamorphism, and exhumation ages of orthogneiss from the SW Sulu terrane (eastern China): SHRIMP U–Pb dating of mineral inclusion-bearing zircons. Lithos 78 (4), 411–429.
Liu, D.Y., Jian, P., Kroner, A., Xu, S.T., 2006. Dating of prograde metamorphic events deciphered from episodic zircon growth in rocks of the Dabie–Sulu UHP complex, China. Earth and Planetary Science Letters 250 (3–4), 650–666.
Liu, Y.S., Zong, K.Q., Kelemen, P.B., Gao, S., 2008. Geochemistry and magmatic history of eclogues and ultramafic rocks from the Chinese continental scientific drill hole: subduction and ultrahigh-pressure metamorphism of lower crustal cumulates. Chemical Geology 247 (1–2), 133–153.
Ma, J.L., Wei, G.J., Xu, Y.G., Long, W.G., Sun, W.D., 2007. Mobilization and re-distribution of major and trace elements during extreme weathering of basalt in Hainan Island, South China. Geochimica Et Cosmochimica Acta 71, 3223–3237.
McDonough, W.F., 1991. Partial melting of subducted oceanic-crust and isolation of its residual eclogitic lithology. Philosophical Transactions of the Royal Society of London Series A – Mathematical Physical and Engineering Sciences 335 (1638), 407–418.
McDonough, W.F., Sun, S.S., 1995. The composition of the Earth. Chemical Geology 120 (3–4), 223–253.
Meng, Q.R., Zhang, G.W., 1999. Timing of collision of the North and South China blocks: controversy and reconciliation. Geology 27 (2), 123–126.
Meng, Q.R., Zhang, G.W., 2000. Geologic framework and tectonic evolution of the Qinling orogen, central China. Tectonophysics 323 (3–4), 183–196.
Munker, C., Pfander, J.A., Weyer, S., Buchl, A., Kleine, T., Mezger, K., 2003. Evolution of planetary cores and the earth–moon system from Nb/Ta systematics. Science 301 (5629), 84–87.
Munker, C., Worner, G., Yogodzinski, G., Churikova, T., 2004. Behaviour of high field strength elements in subduction zones: constraints from Kamchatka–Aleutian arc lavas. Earth and Planetary Science Letters 224 (3–4), 275–293.
Niu, Y.L., Batiza, R., 1997. Trace element evidence from seamounts for recycled oceanic crust in the eastern Pacific mantle. Earth and Planetary Science Letters 148 (3–4), 471–483.
Oberti, R., Vannucci, R., Zanetti, A., Tiepolo, M., Brumm, R.C., 2000. A crystal chemical re-evaluation of amphibole/melt and amphibole/clinopyroxene D–Ti values in petrogenetic studies. American Mineralogist 85 (3–4), 407–419.
Pearce, N.J.G., Perkins, W.T., Westgate, J.A., Gorton, M.P., Jackson, S.E., Neal, C.R., Chenery, S.P., 1997. A compilation of new and published major and trace element data for NIST SRM 610 and NIST SRM 612 glass reference materials. Geostandards Newsletter – The Journal of Geostandards and Geoanalysis 21 (1), 115–144.
Prowatke, S., Klemme, S., 2005. Effect of melt composition on the partitioning of trace elements between titanite and silicate melt. Geochimica Et Cosmochimica Acta 69 (3), 695–709.
Rapp, R.P., Watson, E.B., Miller, C.F., 1991. Partial melting of amphibolite eclogite and the origin of archean trondhjemites and tonalites. Precambrian Research 51, 1–25.
Rapp, R.P., Shimizu, N., Norman, M.D., 2003. Growth of early continental crust by partial melting of eclogite. Nature 425 (6958), 605–609.
Rudnick, R.L., 1995. Making continental-crust. Nature 378, 571–578.
Rudnick, R.L., Barth, M., Horn, I., McDonough, W.F., 2000. Rutile-bearing refractory eclogites: missing link between continents and depleted mantle. Science 287 (5451), 278–281.
Schmidt, M.W., Dardon, A., Chazot, G., Vannucci, R., 2004. The dependence of Nb and Ta rutile-melt partitioning on melt composition and Nb/Ta fractionation during subduction processes. Earth and Planetary Science Letters 226 (3–4), 415–432.
Shannon, R.D., 1976. Revised effective ionic-radii and systematic studies of interatomic distances in halides and chalcogenides. Acta Crystallographica Section, A 32, 751–767.
Stalder, R., Foley, S.F., Brey, G.P., Horn, I., 1998. Mineral aqueous fluid partitioning of trace elements at 900–1200 degrees C and 3.0–5.7 GPa: new experimental data for garnet, clinopyroxene, and rutile, and implications for mantle metasomatism. Geochimica Et Cosmochimica Acta 62 (10), 1781–1801.
Sun, S.S., McDonough, W.F., 1989. Chemical and isotopic systematics of oceanic basalts; Implications for mantle composition and processes. Magmatism in the Ocean Basins, 42. Geological Society of London, London.
Sun, W.D., Li, S.G., Chen, Y.D., Li, Y.J., 2002a. Timing of synorogenic granitoids in the South Qinling, central China: constraints on the evolution of the Qinling–Dabie orogenic belt. Journal of Geology 110 (4), 457–468.
Sun, W.D., Williams, I.S., Li, S.G., 2002b. Carboniferous and Triassic eclogites in the western Dabie Mountains, east-central China: evidence for protracted convergence of the North and South China Blocks. Journal of Metamorphic Geology 20 (9), 873–886.
Sun, W.D., Bennett, V.C., Eggins, S.M., Arculus, R.J., Perfit, M.R., 2003. Rhenium systematics in submarine MORB and back-arc basin glasses: laser ablation ICP-MS results. Chemical Geology 196 (1–4), 259–281.
Sun, X.M., Tang, Q., Sun, W.D., Xu, L., Zhai, W., Liang, J.L., Liang, Y.H., Shen, K., Zhang, Z.M., Zhou, B., Wang, F.Y., 2007. Monazite, iron oxide and barite exsolutions in apatite aggregates from CCSD drillhole eclogites and their geological implications. Geochimica Et Cosmochimica Acta 71 (11), 2896–2905.
Tiepolo, M., Vannucci, R., Oberti, R., Foley, S., Bottazzi, P., Zanetti, A., 2000. Nb and Ta incorporation and fractionation in titanian pargasite and kaersutite: crystal–chemical constraints and implications for natural systems. Earth and Planetary Science Letters 176 (2), 185–201.
Tiepolo, M., Bottazzi, P., Foley, S.F., Oberti, R., Vannucci, R., Zanetti, A., 2001. Fractionation of Nb and Ta from Zr and Hf at mantle depths: the role of titanian pargasite and kaersutite. Journal of Petrology 42 (1), 221–232.
Tiepolo, M., Oberti, R., Vannucci, R., 2002. Trace-element incorporation in titanite: constraints from experimentally determined solid/liquid partition coefficients. Chemical Geology 191 (1–3), 105–119.
Tu, X.L., Zhang, H.F., Deng, W.F., Liang, H.Y., Sun, W.D., in press. Application of RESOlution laser ablation ICPMS in trace element analyses. Geochimica.
Wade, J., Wood, B.J., 2001. The Earth's 'missing' niobium may be in the core. Nature 409 (6816), 75–78.
Wang, X.M., Liou, J.G., 1991. Regional ultrahigh-pressure coesite-bearing eclogitic terrane in Central China – evidence from country rocks, gneiss, marble, and metapelite. Geology 19 (9), 933–936.
Wang, X.M., Liou, J.G., Mao, H.G., 1989. Coesite-bearing eclogites from Dabie Mountains in central China. Geology 17, 1085–1088.
Xiao, Y.L., Sun, W.D., Hoefs, J., Simon, K., Zhang, Z.M., Li, S.G., Hofmann, A.W., 2006. Making continental crust through slab melting: constraints from niobium–tantalum fractionation in UHP metamorphic rutile. Geochimica Et Cosmochimica Acta 70 (18), 4770–4782.
Xiong, X.L., Adam, J., Green, T.H., 2005. Rutile stability and rutile/melt HFSE partitioning during partial melting of hydrous basalt: implications for TTG genesis. Chemical Geology 218 (3–4), 339–359.
Xiong, X.L., Adam, J., Green, T.H., Niu, H.C., Wu, J.H., Cai, Z.Y., 2006. Trace element characteristics of partial melts produced by melting of metabasalts at high pressures: constraints on the formation condition of adakitic melts. Science in China Series D-Earth Sciences 49 (9), 915–925.
Xu, Z.Q., 2004. The scientific goals and investigation progresses of the Chinese Continental Scientific Drilling Project. Acta Petrologica Sinica 20 (1), 1–8.
Xu, Z.Q., 2007. Continental deep subduction and exhumation dynamics: evidence from the main hole of the Chinese Continental Scientific Drilling and the Sulu HP-UHP metamorphic terrane. Acta Petrologica Sinica 23 (12), 3041–3053.
Xu, S.T., Okay, A.I., Ji, S.Y., Sengor, A.M.C., Wen, S., Liu, Y.C., Jiang, L.L., 1992. Diamond from the Dabie–Shan metamorphic rocks and its implication for tectonic setting. Science 256 (5053), 80–82.
Xu, S.T., Liu, Y.C., Chen, G.B., Compagnoni, R., Rolfo, F., He, M.C., Liu, H.F., 2003. New finding of micro-diamonds in eclogites from Dabie–Sulu region in central-eastern China. Chinese Science Bulletin 48 (10), 988–994.
Xu, J., Chen, Y.C., Wang, D.H., Yu, J.J., Li, C.J., Fu, X.J., Chen, Z.Y., 2004. Titanium mineralization in the ultrahigh-pressure metamorphic rocks from Chinese Continental Scientific Drilling 100 similar to 2000 m main hole. Acta Petrologica Sinica 20 (1), 119–126.
Xu, Z.Q., Yang, J.S., Zhang, Z.M., Liu, F.L., Wang, R.C., Luo, L.Q., Huang, L., Dong, H.L., 2005. Completion and achievements of Chinese Continental Scientific Drilling (CCSD) Project. Geology in China 32, 177–182.
Ye, K., Cong, B.L., Ye, D.I., 2000. The possible subduction of continental material to depths greater than 200 km. Nature 407 (6805), 734–736.
Yuan, H.L., Gao, S., Liu, X.M., Li, H.M., Günther, D., Wu, F.Y., 2004. Accurate U–Pb age and trace element determinations of zircon by laser ablation-inductively coupled plasma mass spectrometry. Geoanalytical and Geostandard Research 28 (3), 353–370.
Zack, T., Kronz, A., Foley, S.F., Rivers, T., 2002. Trace element abundances in rutiles from eclogites and associated garnet mica schists. Chemical Geology 184 (1–2), 97–122.
Zhang, R.Y., Liou, J.G., Yang, J.S., Ye, K., 2003. Ultrahigh-pressure metamorphism in the forbidden zone: the Xugou garnet peridotite, Sulu terrane, eastern China. Journal of Metamorphic Geology 21 (6), 539–550.
Zhang, Z.M., Xu, Z.Q., Liu, F.L., You, Z.D., Shen, K., Yang, J.S., Li, T.F., Chen, C.Z., 2004. Geochemistry of eclogites from the main hole (100 similar to 2050 m) of the Chinese Continental Scientific Drilling Project. Acta Petrologica Sinica 20 (1), 27–42.
Zhang, Z.M., Shen, K., Sun, W.D., Liu, Y.S., Liou, J.G., Shi, C., Wang, J.L., 2008. Fluids in deeply subducted continental crust: petrology, mineral chemistry and fluid inclusion of UHP metamorphic veins from the Sulu orogen, eastern China. Geochimica Et Cosmochimica Acta 72 (13), 3200–3228.
Zheng, Y.F., Fu, B., Gong, B., Li, L., 2003. Stable isotope geochemistry of ultrahigh pressure metamorphic rocks from the Dabie–Sulu orogen in China: implications for geodynamics and fluid regime. Earth-Science Reviews 62 (1–2), 105–161.